2014

Biogeochemistry of Sulfur Isotopes in Crystal Lake, Clark County, West-Central Ohio

Amanda Lynn Meyer
Wright State University

BIOGEOCHEMISTRY OF SULFUR ISOTOPES IN CRYSTAL LAKE, CLARK COUNTY, WEST-CENTRAL OHIO

A thesis submitted in partial fulfillment of the requirements for the degree of Master of Science

By

AMANDA LYNN MEYER
B.A., Miami University, 2011

2014
Wright State University

WRIGHT STATE UNIVERSITY

GRADUATE SCHOOL

December 12th, 2014

I HEREBY RECOMMEND THAT THE THESIS PREPARED UNDER MY SUPERVISION BY Amanda Lynn Meyer ENTITLED Biogeochemistry of Sulfur Isotopes in Crystal lake, Clark County, West-Central Ohio. BE ACCEPTED IN PARTIAL FULFILLMENT OF THE REQUIREMENTS FOR THE DEGREE OF Master of Science.

Songlin Cheng, Ph.D.
Thesis Director

David F. Dominic, Ph.D.
Chair, Department of Earth & Environmental Sciences

Committee on
Final Examination

Rebecca Teed, Ph.D.

Chad Hammerschmidt, Ph.D.

Songlin Cheng, Ph.D.

Robert E. W. Fyffe, Ph.D.
Vice President for Research and
Dean of the Graduate School

ABSTRACT

Meyer, Amanda Lynn. M.S. Department of Earth and Environmental Sciences, Wright State University, 2014. Biogeochemistry of Sulfur Isotopes in Crystal Lake, Clark County, West-central Ohio.

Crystal Lake showed distinct biogeochemical patterns, which were governed by thermal stratification, photosynthesis, and sulfur redox processes. Field parameter measurements and water and *Planktothrix rubescens* samples were collected in May, August, and October, 2013 at the deepest point in the lake, to better understand these processes. At the metalimnion–hypolimnion boundary, *P. rubescens* produced chlorophyll and turbidity maxima. Photosynthesis produced oxygen-rich and nutrient-poor surface waters. The decay of organic matter produced anoxic, nutrient-rich water in the hypolimnion. Sulfate concentrations were high in the epilimnion and metalimnion, with a maximum at the layer of *P. rubescens*, and decreased with depth in the hypolimnion. Sulfide was absent in the epilimnion and metalimnion and increased with depth in the hypolimnion. Sulfur isotopic composition changed with depth in the hypolimnion due to Rayleigh Fractionation. It can be concluded that *P. rubescens* play a major role in the sulfur cycle and sulfur isotopic composition changes.

TABLE OF CONTENTS

TABLE OF CONTENTS (Continued)

Page

TABLE OF CONTENTS (Continued)

Page

TABLE OF CONTENTS (Continued)

Page

LIST OF FIGURES

LIST OF FIGURES (Continued)

Figure Page

LIST OF TABLES

LIST OF TABLES (Continued)

Page

I. INTRODUCTION AND PURPOSE

EUTROPHICATION

Eutrophication is the result of nutrient enrichment in natural waters, which affects the production of aquatic organisms (Yang et al., 2008). There are different levels of eutrophication that depend on the amount of nutrient concentration. Nitrogen (N) and phosphorus (P) are the two main nutrients leading to eutrophication that are utilized during photosynthesis reactions such as that described by the Redfield equation (Eq. 1).

$$106CO_2 + 16NO_3 + HPO_4^{2-} + 122H_2O + 18H^+ + \text{Energy \& Micronutrients}$$
$$\rightarrow C_{106}H_{263}O_{110}N_{16}P \text{ (algal biomass)} + 138O_2 \qquad \text{(Eq. 1)}$$

Consequences of eutrophication are the amount of primary production, a loss of lake clarity, and hypoxia. Dissolved oxygen (DO) is consumed when algal biomass is respired by photosynthetic organisms. The decomposition of dead organisms in the hypolimnion also removes DO from the water column (Smith et al., 1999).

Nutrient cycles are altered due to the increase of human activities. Use of fertilizer, burning of fossil fuels, and waste pollution has increased the amount of nutrient input into terrestrial and aquatic ecosystems. Nutrient runoff from terrestrial regimes often results from either fertilizer use, inadequate wastewater treatment, or use of soaps and detergents. Nutrient-laden runoff flows into rivers and then into lakes and oceans (Smith et al., 1999, EPA.gov, 2014). The burning of fossil fuels adds nutrients to lake systems due to oxidation of the sulfur and nitrous oxides in the atmosphere as they react

with water and are then wet deposited. Due to this increase of nutrients in lake systems, algal growth has flourished in many lakes.

Many Ohio lakes are experiencing hyper-eutrophication. Grand Lake St. Mary's (GLSM), in West-Central Ohio, is one such lake. GLSM has undergone extreme eutrophication not only due the nutrient runoff, but also due to the high surface-area to depth ratio of the lake. The morphometry of the basin allows for nutrients to be readily recycled between the benthos and photic zone where they can be used to drive primary production. Accordingly, GLSM has the highest microcystin concentration in Ohio due to eutrophication. Some cyanobacteria produce microcystin to prevent grazing, making them more competitive among other phytoplankton. Eutrophication causes an excess of P in the surface waters, but there may not be an ample amount of N input, causing N limitation for cyanobacteria. Another possible use of microcystin in cyanobacteria is N replacement in this circumstance (Figueiredo, 2004).

Lake Erie also has been eutrophied since the mid 1990's (Scavia et al., 2014). High levels of cyanobacteria mass are indicative of eutrophication, along with hypoxia developing in deep waters of the central basin of the lake. Cyanobacteria blooms and hypoxia are symptoms of eutrophication caused by a dramatic increase in dissolved reactive phosphorus concentrations in Lake Erie tributaries (Scavia et al., 2014). A recent increase of microcystin in Buckeye Lake has been a major concern due to blooms of blue-green algae (Arenschield, 2014). Buckeye Lake is another example of eutrophication occurring in Ohio's natural freshwater systems. Eutrophication in Ohio freshwater lakes does not only affect the state, but downstream regions as well. Water from many of Ohio's lakes drains to either Lake

Erie or the Ohio River, which flows into the Mississippi River and eventually the Gulf of Mexico. During the summer, an area of hypoxic water, termed the "Dead Zone", is observed in the northern Gulf of Mexico. This zone of hypoxia is a result of nutrient-rich water entering the Gulf from the Mississippi and Atchafalaya Rivers (Rabalais et al., 2002).

SULFUR

The biogeochemical cycling of sulfur can be exacerbated by eutrophication creating extreme oxidation-reduction gradients. Common forms of sulfur in freshwater aquatic environments are sulfate (SO_4^{2-}) and sulfide (S^{2-}) (Dahl et al., 2008). The relative concentrations of sulfate and sulfide are dependent on the oxidation-reduction conditions of the water column (Cheng, 2014).

Sulfur can originate from natural and anthropogenic sources and can occur in the atmosphere, biosphere, hydrosphere and lithosphere in solid, liquid and gaseous forms. Natural sources and reservoirs of sulfur include: weathering of geologic materials, fossil fuel combustion, peat and soil, plants, humans and animals. Many man-made facilities emit gaseous sulfur dioxide (SO_2) into the atmosphere by fossil fuel combustion. Sulfur dioxide reacts with hydrogen peroxide in the atmosphere to form sulfuric acid (O'Brien and Birkner, 1977). This acid can be deposited as wet deposition, such as rain, snow, or fog, or as dry deposition on fine particles. Approximately two-thirds of all atmospheric SO_2 in the United States originates from the burning of fossil fuels. These emissions have dramatically decreased during the past two decades, from about 1.4 million tons in 1998 to around 350,000 tons in 2012, due to the enactment of the Clean Air Act of 1970 and

the Clean Air Act amendments of 1990. The decline in SO_2 emissions is a result of scrubbers that eliminate pollutants from power plant exhaust gases (Stewart, 2008). Sources of sulfur to lakes are most often attributed to groundwater, wet and dry atmospheric deposition, runoff, and mobilization from bottom sediments (Hicks, 2007).

Sulfate is an abundant and significant sulfur compound in freshwater lakes and an important source of sulfur for aquatic biota. In oxic environments, reduced sulfur compounds can readily be oxidized to sulfate (Dahl et al., 2008). Acid rain deposition to freshwater lakes may result in accumulation of SO_4^{2-} throughout the water column due to Eq. 2 (Jedrysek, 2005).

$H_2SO_4 + H_2O \rightarrow H_3O^+ + HSO_4^-$ $K_1 = 2.4 \times 10^6$ (Eq. 2)

$HSO_4^- + H_20 \rightarrow H_30^+ + SO_4^{2-}$ $K_2 = 1.0 \times 10^{-2}$

Sulfate accumulation has decreased in freshwater lakes by approximately 50% between 1989 and 2009 due to the Clean Air Act (epa.gov, 2009). This may result in sulfur becoming a limiting factor for phytoplankton growth in some freshwater systems (Dahl et al., 2008). One such example is an oligotrophic lake in northern England, where, prior to 1970, sulfate and phosphorus input into the system allowed phytoplankton to replenish (Hell, 2008). The decline in SO_2 emissions could eventually result in sulfur becoming the limiting factor of these phytoplankton directly or by decreasing the influence of the mineralization of iron sulfides on the availability of phosphorus (Hell, 2008).

Lakes that are relatively deep compared to the total surface area often have an anoxic hypolimnion where sulfide can accumulate to high concentrations. Sulfide sources

in the hypolimnion include dissolution of minerals in the sediments and microbial sulfate reduction. Sulfur is highly reactive in its reduced forms, such as S^{2-} (Dahl et al., 2008).

SULFER CYCLING MICROORGANISMS

Microorganisms strongly influence sulfur biogeochemistry (Hell, 2008). Previously, vertical profiles of Crystal Lake, West-Central Ohio, have shown maximum concentrations of chlorophyll and turbidity at the boundary between the meta- and hypolimnions. These maxima were due to a concentrated layer of purple sulfur bacteria (PSB) that have been identified microscopically (Sadurski, 2012). PSB are anoxygenic photosynthesizers that utilize sulfide as the electron donor for cellular growth to create globules of elemental sulfur (S^0) inside the cell (Eq. 3).

$$6CO_2 + 12H_2S + \text{Sunlight} \rightarrow C_6H_{12}O_6 \text{ (carbon chains)} + 6H_2O + 12S^0 \quad \text{(Eq. 3)}$$

$$18CO_2 + 12S^0 + 30H_20 \rightarrow 3\ C_6H_{12}O_6 + 12H_2SO_4$$

$$24CO_2 + 12H_2S + 24H_2O \rightarrow 4C_6H_{12}O_6 + 12H_2SO_4$$

The PSB then oxidize the elemental sulfur to sulfate as it is released from the cell (Gemerden, 1995; Eq. 3). During this initial study, *Planktothrix rubescens* was identified at this boundary, between the metalimnion and hypolimnion, instead of PSB.

In my initial investigations of Crystal Lake, *Planktothrix rubescens*, which is not a PSB, was identified at the boundary between the metalimnion and hypolimnion. *P. rubescens* is a reddish cyanobacteria that is planktonic in and common in freshwater lakes of central, northern, and northeastern Europe as well as the northeastern U.S. (Komárek & Komárková, 2004). *P. rubescens* require little light for photosynthesis and

can tolerate a greater range of temperatures than most other cyanobacteria, allowing them to survive at greater depths (Halstvedt et al., 2007). There is less competition for nutrients and other resources at the metalimnion-hypolimnion boundary than in surface waters where most phytoplankton and other microorganisms thrive. Colonies of *P. rubescens* commonly form in the beginning and final stages of eutrophication in lakes (Lampert and Sommers, 1997). One lake in particular, Lake Zurich, showed a disappearance of these blooms as eutrophication increased due to an increase in algal biomass in the epilimnion and a resulting decrease in transparency (Legnani et al., 2005). *P. rubescens* began reappearing once lake water quality improved as a result of improved wastewater treatment, decreasing the density of algal mass and phosphorus concentrations in the epilimnion (Lampert and Sommers, 1997; Legnani et al., 2005).

P. rubescens were previously classified under the *Oscillitoria* genus. Many oscillitorioids are known to photosynthesize anaerobically in sulfide-rich environments, easily using H_2S as an electron donor instead of H_2O due to the high reactivity of sulfide (Chaudhary et al., 2009). This reaction produces S^0 (Eq. 3). Some oscillitorioids can readily switch back and forth between aerobic and anaerobic photosynthesis (Garlick et al., 1977).

P. rubescens also can produce microcystins, which are cyanotoxins that are harmful to plants and animals (Christiansen, 2008). Microcystins bioaccumulate in fish and other organisms and are harmful to animals and humans by either direct ingestion of the cyanobacteria or indirectly by ingestion of fish and other organisms that have been contaminated (Christiansen, 2008). *P. rubescens* are gaining attention due to their presence in freshwater lakes that are used for recreational purposes and for having the

most cyanotoxin per biomass compared to other toxic cyanobacteria (Halstvedt et al., 2007). Zooplankton typically avoid grazing on *P. rubescens* as a result of the microcystin, facilitating the growth and competitive nature of *P. Rubescens* (Figueiredo, 2004).

P. rubescens, and other oscillitoroids, contain gas vesicles that allow for buoyancy regulation (Figure 1). Buoyancy regulation is necessary to offset molecules within the cell that are denser than water and for the phytoplankton to stratify in the water column under ideal light and nutrient conditions (Konopka et al., 2003; Legnani et al., 2005). *P. rubescens* generally thrive in regions of freshwater lakes where reactive PO_4^3—P concentrations range 0--10 µg P l^{-1} (Legnani et al., 2005). The ability of *P. rubescens* to 1) survive in low light and temperatures, 2) produce microcystins, and 3) regulate buoyancy makes it more competitive among many other phytoplankton. Bacterial attachment is rarely observed with these *P. rubescens*, suggesting that colonization is resisted (Van den Wyngaert et al., 2011).

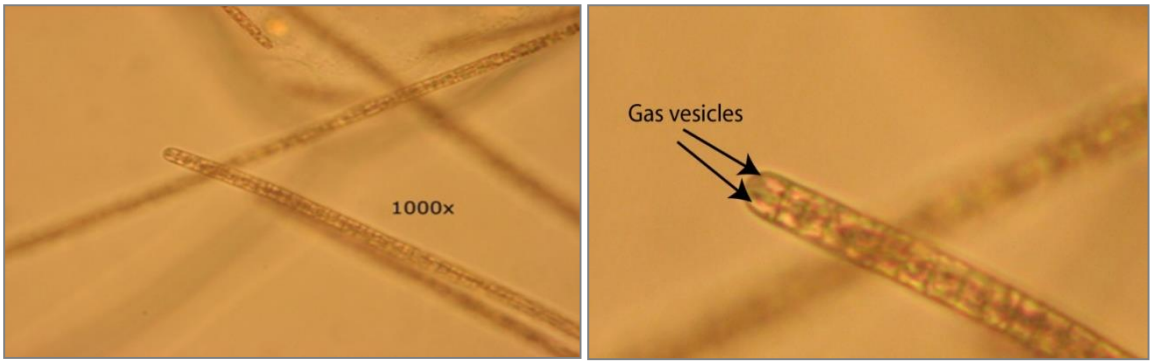

Figure (1). a. Representative image at 1000x magnification of filamentous *P. rubescens* found at 5.9 m depth. The filaments range in size from approximately 825 to 2500 micrometers in length and are all about 5 micrometers wide. Filaments were entwined as a mass. **b**. Arrows point to gas vacuoles that alter the buoyancy of the cyanobacteria (Konopka, 2013).

Another group of microorganisms present within Crystal Lake is sulfate-reducing bacteria. These bacteria reduce sulfate to sulfide under anoxic conditions. Sulfate-

reducing bacteria are the most likely cause of the strongly reducing conditions produced in the hypolimnion due to respiration processes consuming O_2.

SULFUR ISOTOPES

Biogeochemical reactions and transformations of sulfur, and other constituents affected by microbial mediation, cannot be recognized solely through chemical concentration analyses: stable isotopic measurements must also be made (Jedrysek, 2005). Large relative differences in mass between each isotope of a light element lead to differences in reaction rates. This affects the isotopic composition, as fractionation occurs during various physiochemical and biological processes (Clark and Fritz, 1997). Lighter isotopes react more quickly than heavier isotopes due to the stronger molecular bonds of the heavy nuclei. Far more energy is required to break stronger bonds, or detach them from the "comfort zone", which is essential for reaction to occur. The higher energy requirement needed to break the stronger bonds of the heavy isotopes generally produces a heavier isotopic condensed phase, such as the aqueous phase in a vapor-liquid reaction.

Sulfur has four stable isotopes, with the most abundant being ^{34}S and ^{32}S.

- 32S: 95.02 %
- 33S: 0.75 %
- 34S: 4.21 %
- 36S: 0.02 % (Hoefs, 1987)

The abundance ratio of [$^{34}S/^{32}S$] of a sample is measured relative to the standard reference material, CDT troilite from the Canyon Diablo meteorite, which has an abundance ratio of 0.0450 (de Groot, 2004). This relationship is expressed as follows:

$$\delta^{34}S(‰) = \left\{ \frac{[\frac{^{34}S}{^{32}S}]_{sample}}{[\frac{^{34}S}{^{32}S}]_{standard}} - 1 \right\} x\ 1000\ ‰ \qquad \text{(Eq. 4)}$$

[$^{34}S/^{32}S$] is defined as the ratio of ^{34}S atoms to ^{32}S atoms in the sample and standard materials. Precise determinations of this ratio in the samples can be attained in a variety of ways, depending on the research objective (de Groot, 2004). Determination of the abundance ratio can be useful in determining the source of sulfur. For example, sulfate which is derived from sulfide, will typically be isotopically lighter than if it had come from another source.

PURPOSE OF STUDY

The purpose of this study was to identify the vertical distribution and seasonal variation of the isotopic composition of SO_4^{2-} and S^{2-} in Crystal Lake. Currently there are no sulfur isotopic composition transformation measurements by either PSB or *P. rubescens* in the literature and no systematic studies of the impact of fractionation between sulfate and sulfide with either PSB or *P. rubescens* as a mediator. Previously, the goal was to identify the sulfur isotope composition of the PSB at the metalimion/hypolimnion boundary, because it could reveal the potential role of PSB in affecting the sulfur biogeochemistry in the lake. It was hypothesized that PSB would increase sulfate concentrations and decrease the $\delta^{34}S_{sulfate}$ ratio at this layer. However, *P. rubescens* was identified instead of PSB. Therefore the hypothesis was revised to include *P. rubescens* instead of PSB as the cause of a sulfate concentration increase and decrease in $\delta^{34}S_{sulfate}$ ratio.

II. MATERIALS AND METHODS

STUDY SITE

Crystal Lakes are a sequence of four interconnected lakes located in southwest Clark County in west-central Ohio. Main Lake, a.k.a. Crystal Lake, is the largest and deepest among the lakes, with a surface area of about 52000 m^2, a maximum depth of 11.9 m , and mean depth of 3.8 m (Woodruff, 1999; Figure 2). Crystal Lake has a volume of approximately 200,000m^3.

Crystal Lake is the southernmost glacial lake in southwest Ohio (Woodruff 1999). The bedrock beneath Crystal Lake is composed of Ordovician dolomitic limestone inter-bedded with calcareous shale (Woodruff 1999). The base of Crystal Lake is composed of a sand and gravel buried valley of outwash produced by the Wisconsin glaciation (Norris, 1952). Crystal Lakes were formed 15,000-12,000 years ago when a Wisconsinan glacier retreated. The Miami buried valley and outwash plain were formed by the Teays drainage system (Goldthwait 1952). Based on the linear distribution of the lakes of Crystal Lakes, they are most likely Moulin-induced glacial lakes (Cheng 2014).

Recently, the lake has been classified as mesotrophic based on secchi disk and phosphorus concentration measurements, a shift from the eutrophic classification it had maintained since 1975 (Talsna and Lazorchak, 1975). Thermal stratification,

photosynthesis, and decomposition of organic material in the bottom sediments control the biogeochemistry of the lake. Dissolved oxygen and nutrients are mixed throughout the lake twice a year. Thermal stratification develops after spring turnover around May with similar mixing patterns in each year. The lakes are stream-fed from the north and flow into the Mad River to the south (Wisebaker, 2008). The watershed is composed of agricultural and residential land and the lake is used for recreation (Talsna and Lazorchak, 1975). Houses near the lake are connected to a sewage system (Collins, 1999).

In many natural freshwater lakes, pelagic and attached algae are dominant photosynthesizers. *Planktothrix rubescens* cyanobacteria were found at Crystal Lake during my initial study, but other photosynthesizers, such as green algae and diatoms, are either likely or known to be present. A systematic study of the different algal species has not been conducted in Crystal Lake, but it is common to find these species in natural waters in the area.

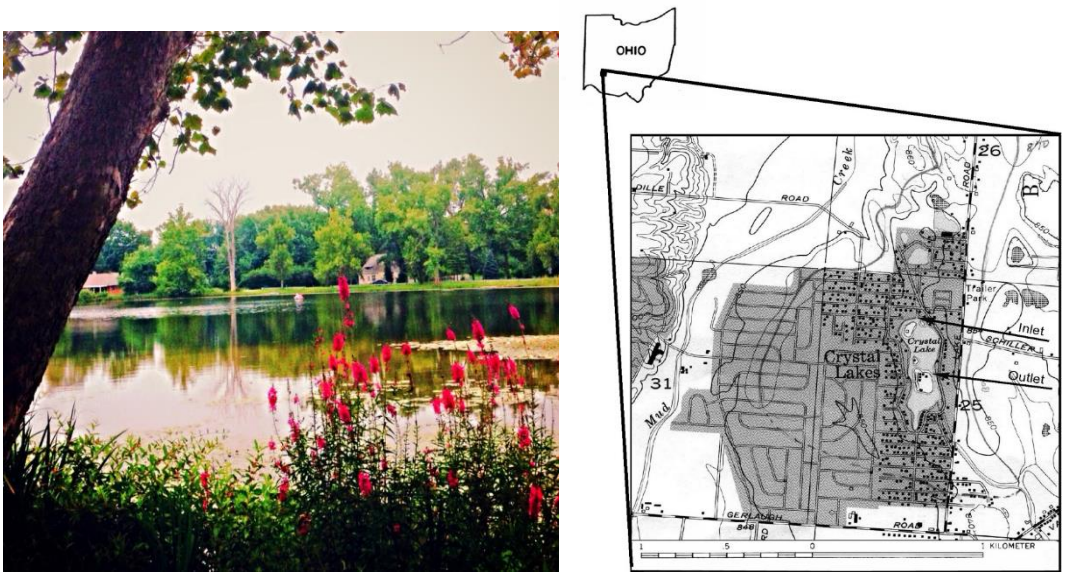

Figure 2. a.) Image of Crystal Lake b.) A map of the region.

FIELD PARAMETERS

Water quality parameters were vertically profiled (every 0.5 m) at the deepest point in Crystal Lake. Parameters included DO, pH, temperature, specific conductivity, turbidity, chlorophyll, and Eh, measured with either a YSI Sonde 6600 V2 or a YSI Sonde 600 XL. Water was sampled from the same location at 1 m depth intervals through the entire water column in May, August, and October 2013. Nalgene wide-mouth bottles were cleaned with 10% HCl and rinsed with high-quality deionized water before sampling. Samples were filtered through 0.22 µm membranes using a vacuum pump prior to analysis of major anions, alkalinity, phosphorus, sulfide, ammonia, silica, and sulfur isotopes. Sulfide and ammonia were measured colorimetrically immediately upon sampling in the field.

Water samples (250 mL) were transported to Wright State University and kept at 1.6–4.4 ºC until analysis of phosphorus, silica, alkalinity, and major anions. Phosphorus was measured promptly as PO_4^{3-} and converted mathematically to phosphorus (PO_4^{3-}-P). Reactive and total phosphate were analyzed with a phosphorus (total and acid hydrolyzable) TNT reagent set and a Hach DR/4000. Standard phosphorus solutions were prepared at 100, 300, 500, 800, and 1000 ng/l as P. Absorbance was read using Method 3036 at 890 nm. A calibration curve was established using concentration of standards on the Y axis vs. absorbance on the X axis. This curve was then used to determine the concentration of P in each sample. A blank was prepared and its absorbance was subtracted from those of the samples of highly colored waters (Vaccari, 2012).

Silica was determined within two days of sampling with a Hach DR/4000. 2, 4, 6, 8, 10, and 12 mg/L working standard solutions were produced. Calibration curves were established by plotting the concentrations of the working standards on the Y axis vs. the absorbance on the X axis. Sample concentrations were calculated using the R^2 of the calibration curve. 0.5 ml HCl and 1.0 ml AM were added rapidly to 25 ml of sample and mixed. The samples were allowed to react for 5-10 min, then 1.0 ml OA was added and mixed. The absorbance of each sample was then read within 2-15 min at 410 nm. The ratio of H^+:Mo (3.85:1) is important in this procedure for better sensitivity (Vaccari, 2012).

Alkalinity was quantified with a modified Sarazin's Method (Sarazin et al., 1999). Alkalinity standards were produced using a 0.1 M stock. Working standard solutions, from 2-8 mM of alkalinity, were prepared with the stock and suitable dilutions. 4 ml of

formic acid-color indicator solution is added to 2 ml of standard or sample and shaken to outgas CO_2 for analysis. Absorbance is measured at 590 nm with a Hach DR4000. A calibration curve is established using the working standards alkalinity concentration on the Y axis vs. absorbance on the X axis. The best-fit polynomial function is calculated and can then be used to calculate the alkalinity of the samples. A higher concentration of formic acid must be used for samples with higher alkalinity.

Samples were warmed to room temperature and poured into Dionex vials for anion analysis, which was performed using a Dionex ICS-1500. Samples and standards must be filtered with a 0.22 µm membrane prior to analysis. After starting the instrument, the IC must be primed to remove any air bubbles in the tubing. Calibration curves were established by plotting the peak areas on the X axis vs. the concentration of standards on the Y axis. The R^2 value calculated from this curve was used to determine the concentration of specific anions in the samples (Vaccari, 2012).

SULFIDE

Sulfide for isotopic analysis was extracted from lake water by precipitation as insoluble silver sulfide (Ag_2S) based on a method suggested in the USGS report 97–234 (Carmody et al., 1998). Three-liter water samples were collected and samples with greater than 1 mg/L sulfide were treated in the field with an appropriate volume of 10% (wt:vol) silver nitrate ($AgNO_3$), depending on the exact sulfide concentration (Table 1), to precipitate Ag_2S (Carmody et al., 1998). The samples were then transported to Wright State University for filtration of the precipitated mixture of Ag_2S and other silver

compounds. Co-precipitation of silver chloride (AgCl) is likely to occur, therefore, treatment with 3 weight percent ammonium hydroxide (NH_4OH) was required to eliminate other silver compounds and resuspend Cl^- into solution. The Ag_2S precipitate was then filtered again with a 0.22 μm membrane, rinsed, and air-dried for isotopic sulfur analysis.

S^{2-} concentration of sample (mg/L).	mL 10 % $AgNO_3$ solution to add per liter of sample.	Mg Ag_2S produced per liter of sample.	Liters of sample to process to make 39 mg Ag_2S
3.0	0.88	23.2	1.7
2.5	0.73	19.3	2.0
2.0	0.58	15.5	2.5
1.5	0.44	11.6	3.4
1.0	0.29	7.7	5.0
0.5	0.15	3.9	10.1

Table 1. Table 9 of the U.S. Geological Survey Open-File Report 97-234 for direct precipitation of sulfide. Calculations of the amount of $AgNO_3$ to be added to a water sample dependent on concentrations of H_2S.

SULFATE

Sulfate for isotopic analysis was extracted from lake water by precipitation as barium sulfate ($BaSO_4$) based on a method described in the USGS report 97-234 (Carmody et al., 1998). One-liter water samples taken from the hypolimnion, approximately 6 m and deeper were purged with nitrogen (N_2) in the field immediately following collection to evade H_2S. Samples were then transported to the laboratory and filtered with a 0.22 μm membrane. The samples were then acidified to pH 3-4 with dilute, sulfate-free HCl to convert dissolved inorganic carbon (DIC) to carbonic acid (H_2CO_3) to eliminate carbonate (CO_3^{2-}). Barium chloride (BaCl) was then added to precipitate SO_4^{2-}

as barium sulfate ($BaSO_4$) for isotopic analysis. The HCl was added to prevent co-precipitation of barium carbonate ($BaCO_3$) following addition of BaCl. After the $BaSO_4$ had settled overnight, the water samples were again filtered with a 0.22 μm membrane. The precipitate was rinsed with deionized water and centrifuged. The precipitates were then decanted and dried in a desiccator that was sent to the University of Arizona, along with the Ag_2S from the sulfide samples, for sulfur isotopic analysis.

P. RUBESCENS

P. rubescens was sampled from the boundary between the meta- and hypolimnions into 1- and 3-L bottles. *P. rubescens* was filtered from the water onto 0.54 μm membranes pores in the field to concentrate the samples. In the lab, the cyanobacteria were analyzed microscopically to determine the planktonic species, and then dried and powdered for isotopic analysis.

ISOTOPIC ANALYSIS

Isotopic analysis on sulfide, sulfate, and *P. rubescens* samples was performed at the University of Arizona and Northern Arizona University by measurement of $\delta^{34}S$. The University of Arizona measured $\delta^{34}S$ of sulfide and sulfate with SO_2 gas using a ThermoQuest Finnigan Delta PlusXL continuous-flow gas-ratio mass spectrometer (Fry, 2002). A Costech elemental analyzer attached to the mass spectrometer combusted the samples at 1030 °C with a combination of O_2 and V_2O_5. International standards OGS-1 and NBS123 were the basis of standardization of the samples, along with comparison

between sulfide and sulfate materials from other laboratories. Linear calibration occurs between -10 to +30 per mil. Precision of analysis was estimated to be ± 0.15 per mil or better.

It is beneficial to do sulfur isotopic analysis on a variety of sulfur compounds within one system to determine which processes affect the biogeochemistry, therefore the $\delta^{34}S$ of both sulfate and sulfide were studied. Difficulties in sulfur compound extraction commonly reported are: Contamination of one compound with another, isotopic fractionation during aeration, conversion of one compound to another, and insufficient formation of precipitate for isotope ratio mass spectrometry. H_2S, found in reducing environments, can oxidize to sulfate as it is exposed to oxygen during extraction. Therefore, H_2S was precipitated in the field to minimize potential outgassing and oxidation. Dissolved sulfide typically has a $\delta^{34}S$ value over 30 ‰ lower than dissolved sulfate values in the same samples. H_2S was stripped from samples extracted for sulfate analysis to prevent changes in the isotopic composition (de Groot, 2004). S^{2-} from SO_4^{2-} reduction in the hypolimnion should generate isotopically lighter S^{2-} and heavier residual SO_4^{2-}.

III. RESULTS AND DISCUSSION

FIELD PARAMETERS

TEMPERATURE

The biogeochemistry of Crystal Lake is governed by several factors, primarily temperature. The lake was thermally stratified throughout the May–October sampling period (Figure 3a). The epilimnion had similar temperatures between May and August that were warmer than in October, and temperatures in the hypolimnion were relatively constant from the metalimnion-hypolimnion boundary to the bottom during all sampling periods. The thermocline migrated deeper from May to October, and epilimnion-metalimnion and metalimnion-hypolimnion boundaries are indicated by lines colored for each month.

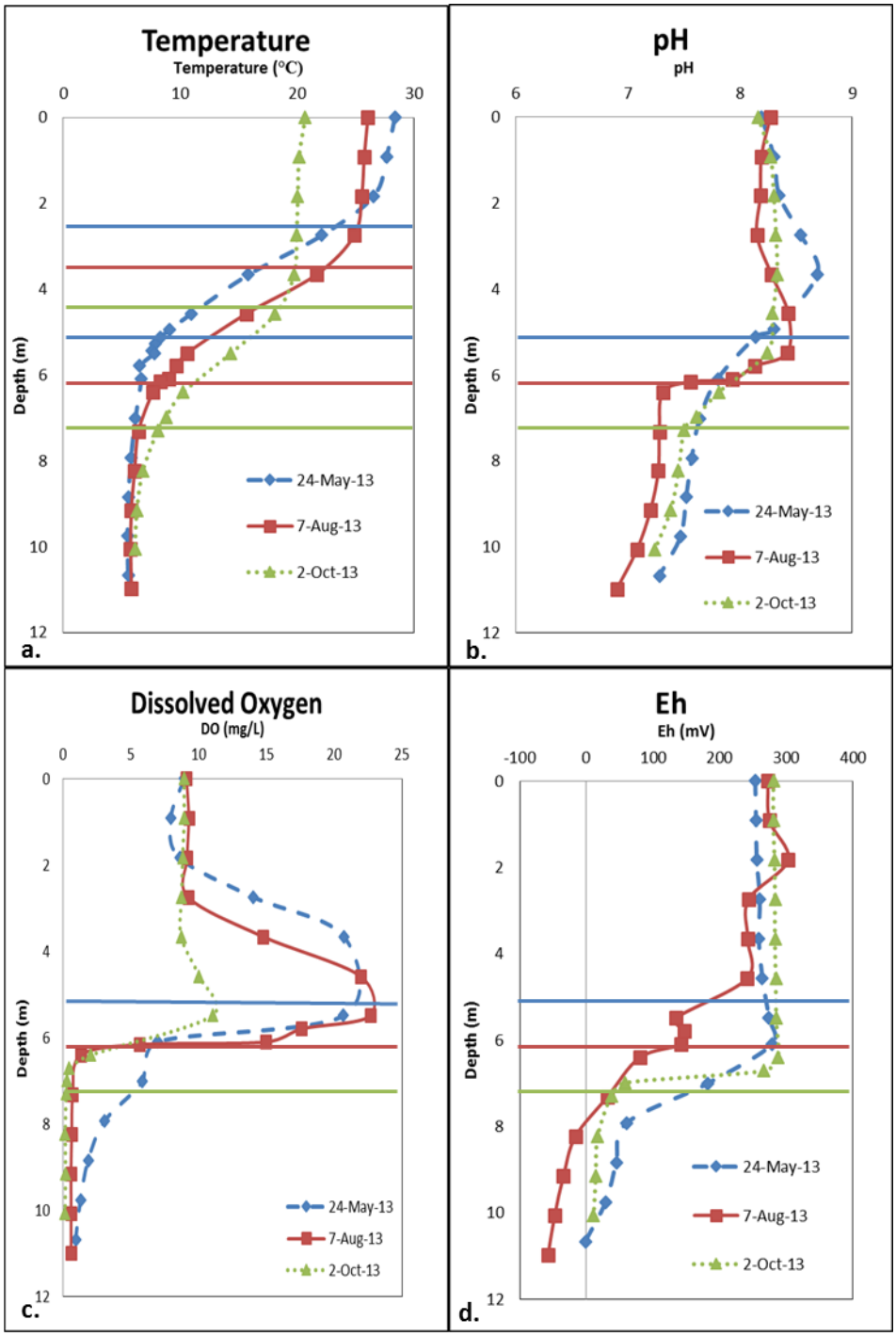

Figure 3. Field parameters collected in May, August and October at Crystal Lake. a. Temperature profiles in °C. b. pH trends. c. Dissolved oxygen concentrations (mg/L). d. Eh trends in mV. The series of blue, red, and green lines indicate monthly thermal stratification boundaries. The colors correspond to the month the line represents. The upper series of lines on the temperature plot indicate the boundary between the epilimnion and metalimnion, and the lower series indicate the boundary between the metalimnion and they hypolimnion. The other plots merely show the metalimnion-hypolimnion boundary.

pH

Crystal Lake had circumneutral pH throughout the water column with more alkaline values in the mixed layer (pH ~8.3 at the surface; Figure 3b). A pH transition zone was observed in the lower metalimnion to lower, more neutral values in the hypolimnion, where a steep decline was observed. A pH maximum was observed in the metalimnion. The maximum was deeper in the water column in August than in May and the October maximum is obscure. The vertical pH distribution followed those of temperature very closely.

Alkalinity buffering in the epilimnion was responsible for the high, constant pH values, as acids are neutralized during this process. If Bicarbonate and carbonate are in the system, they will remove H^+ ions from the water, adding to this increase in pH or stopping a pH decline (Shaw et al., 2004; Eq. 5).

$$CO_3^{2+} + H^+ \leftrightarrow HCO_3^- + H^+ \leftrightarrow H_2CO_3 \leftrightarrow H_2O + CO_2 \quad \text{(Eq. 5)}$$

The pH is correlated to both photosynthesis and decay of organic matter as it is linked to the carbon cycle (Eq. 1, Eq. 5, and Eq. 6). The pH maximum in the metalimnion was due to photosynthesis as the algae consume carbon dioxide (CO_2) (Eq. 1). The decrease in pH in the hypolimnion was a result of respiration and decay of organic matter. As organic matter was decomposed, CO_2 was fluxed back into the hypolimnion and strong acid was released (Eq. 6).

$$C_{106}H_{263}O_{110}N_{16}P \text{ (algal biomass)} + 138O_2 \rightarrow \quad \text{(Eq. 6)}$$

$$106CO_2 + 16NH_4^+ + HPO_4^{2-} + 122H_2O + 2H^+ + \text{Energy \& Micronutrients}$$

DISSOLVED OXYGEN and Eh

Dissovled oxygen was consistently about 9 mg/L in the upper epilimnion (Figure 3c). Subsurface maxima of DO were present within the metalimnion in May and August, with a more obscure maximum in October. The hypolimnion was anoxic in August and October, and DO concentrations were low in May.

The distribution of DO is influenced by temperature, photosynthesis and respiration (Smith et al., 1999). The DO concentrations were relatively homogeneous in the epilimnion where the water was in equilibrium with the atmosphere and wind-driven mixing could occur, causing similar temperatures, and therefore similar DO solubility, throughout this layer. The DO concentrations are slightly lower in this region in May due to higher surface temperatures during this time. As temperature increases, DO solubility decreases (Senese, 1997).

The increase in DO concentration in the metalimnion was due to thermal stratification and photosynthesis. This layer was no longer in equilibrium with the atmosphere as the water got cooler with depth. Photosynthesis within the metalimnion added oxygen to the water (Eq. 1). This increase in DO was accompanied by precipitation of calcium carbonate ($CaCO_3$) as algae consumed CO_2 and pH increased. Due to non-equilibrium conditions, the DO accumulated in the metalimnion as photosynthetic reactions took place. As respiration occurred, oxygen was taken out of the system and carbon dioxide was added, decreasing the pH. During fall and spring turnover, as temperature was fairly homogenous, DO was free to mix throughout the water column.

The Eh values were relatively constant with depth in the epilimnion and metalimnion in May and October, but were more varied in August (Figure 3d). There was

an Eh decline in the hypolimnion in May and October, with values near the sediment-water interface in May being slightly negative and October being close to 0. In August, there was an overall decline from the surface to the bottom sediments, and negative values in the hypolimnion.

Positive Eh values were found in the epilimnion and metalimnion where DO was more abundant, and negative values were observed in the hypolimnion where DO was consumed, particularly under anoxic conditions. The extreme negative values were only found in August due to reduced thermal stratification in May and October.

The temperature profiles in April and May were very different from one another. Thermal stratification was more pronounced in the May profile than the April profile. Temperatures in April ranged between 5 and 14 degrees Celsius, whereas temperatures in May ranged from 5 to 21 degrees Celsius. Dissolved oxygen was present throughout the water column in April, but was only present in May from the surface down to approximately 9 meters producing anoxia in the lower hypolimnion.

Spring turnover occurred in April, disrupting stratification. This turnover mixed DO throughout the water column. Bottom sediments produce sulfide in anaerobic environments, but due to the presence of DO in the hypolimnion during times of mixing, the sulfide would immediately be oxidized to sulfate. DO was absent in May as it was consumed during this process, along with other possible processes (Figure 4).

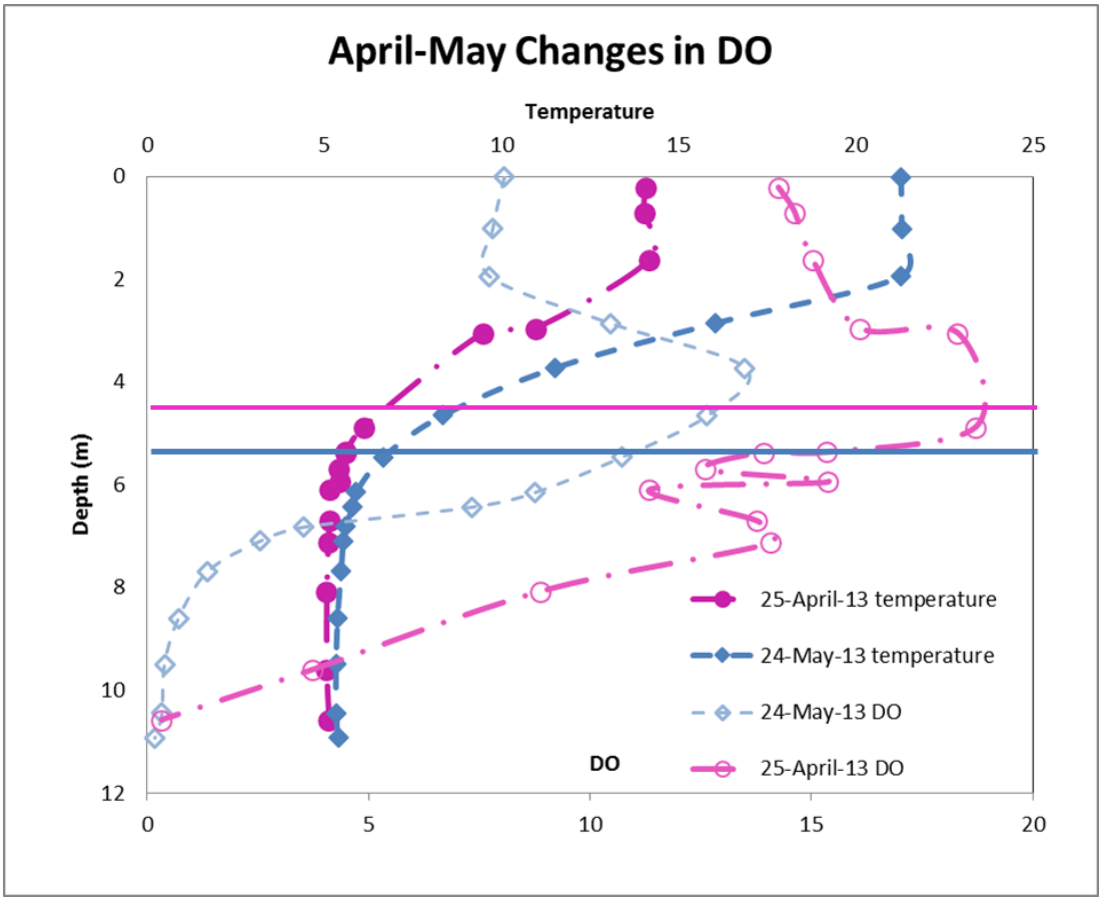

Figure 4. Diagrams showing the difference in thermal stratification and DO concentration between April and May.

CHLOROPHYLL AND TURBIDITY

Chlorophyll concentrations and turbidity in the epilimnion and metalimnion were low, with the exception of a peak at the metalimnion-hypolimnion boundaries and at the water-sediment boundary (Figure 5). Chlorophyll and turbidity maxima of 7 µg/L and 5.9 Nephelometric Turbidity Units (NTUs), respectively, were observed at 5.5 m depth in May. Chlorophyll peaked at 36 µg/L and turbidity peaked at 47.8 NTUs at 6.2 m depth in August. There was a drastic increase in chlorophyll peaking at 219 µg/L around 7.3 m in October. At this same depth turbidity peaked at 31.7 NTUs. Chlorophyll and turbidity concentrations were at maxima at progressively deeper depths each month.

Variations in turbidity and chlorophyll are caused by temperature, light, and nutrient availability. There was an obvious correlation between chlorophyll and turbidity due to the presence of *P. rubescens* at the metalimnion-hypolimnion boundary. The phytoplankton was the main cause of turbidity in the boundary layer in Crystal Lake, along with smaller peaks in turbidity near the bottom of the lake due to resuspension of sediments. Chlorophyll within the cyanobacteria was the cause of the maxima at the metalimnion-hypolimnion boundary. Variation of depth of the maxima and can be attributed to changes in light and nutrient availability, and changes in Eh, due to the requirements for *P. rubescens* survival (Halstvedt et al., 2007). The sulfur species, S^{2-}, is an additional factor potentially responsible for the location of chlorophyll and turbidity peaks, as oscillitoroids, such as *P. Rubescens*, need a source of sulfide for anaerobic photosynthesis (Chaudhary et al., 2009). This will be discussed in detail in the III-4. Sulfate and Sulfide section.

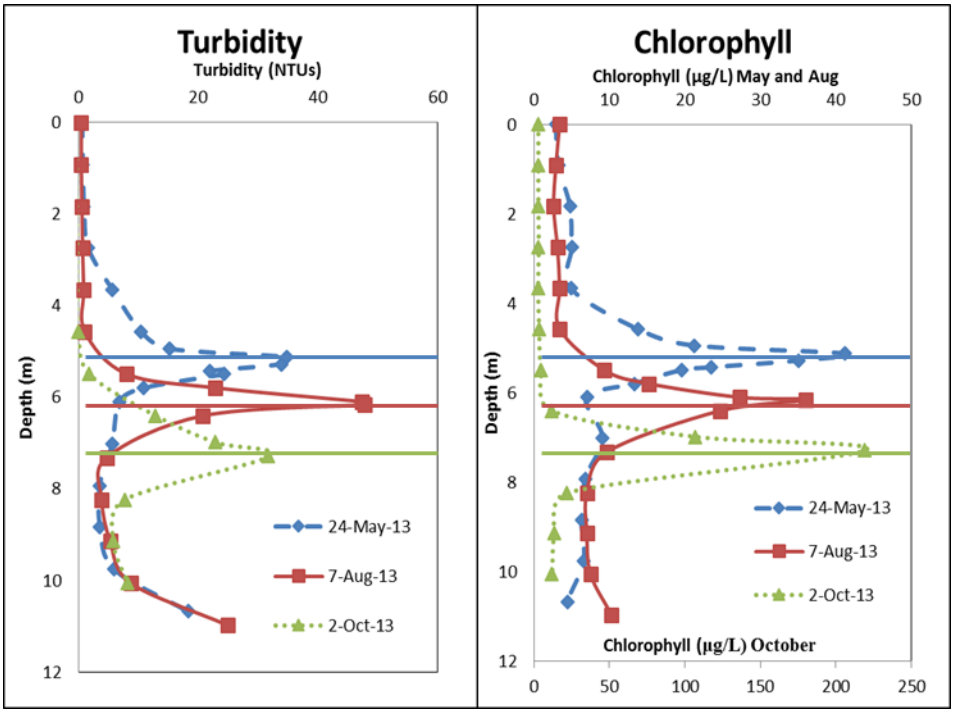

Figure 5. Turbidity and chlorophyll throughout the water column. The metalimnion sinks over time as the surface waters cool, and fall turnover draws near.

CORRELATIONS AMONG FIELD PARAMETERS

There was a strong negative correlation among depth and temperature, pH, and Eh in May (Table 2). Strong correlations were determined as Pearson correlation coefficients +/- 0.7 and above in Table 2. Values between +/- 0.5--0.7 were also significant, to a lesser extent. As depth increased, temperature, pH, and Eh decreased at a similar rate. In May, DO was positively correlated with pH and Eh, and turbidity, chlorophyll, Eh, and pH were also positively correlated with each other. Depth was negatively correlated with temperature and Eh, and positively correlated with turbidity and chlorophyll in August. Temperature was also negatively correlated with turbidity and chlorophyll and positively with Eh. The DO was only positively correlated with pH. Chlorophyll also had a negative correlation with pH and positive correlation with Eh, along with a strong positive correlation with turbidity. The strongest correlations were observed in October. Depth was negatively correlated with temperature, DO and pH, and positively correlated with turbidity and chlorophyll in October. The only parameters that were not strongly correlated during this month were depth and Eh.

As previously described, as depth increased, temperature, pH, and Eh decreased at similar rates. Temperature and Eh decreased with depth as the water column was no longer in equilibrium with the atmosphere during times of thermal stratification. The pH becomes lower with depth, as respiration added more carbon dioxide to the bottom of the water column and increased acidity. DO increased in the metalimnion and decreased in the hypolimnion due to photosynthesis and respiration reactions (Smith et al., 1999).

These reactions were also responsible for changes in pH and Eh which was the reason for the positive correlation between these parameters and DO. The strong correlations among turbidity and chlorophyll were caused by the layer of *P. rubescens*, which were the main contributors of these parameters.

24-May-13								
CORRELATION	Depth	Temperature	DO	pH	Turbidity	Chlorophyll	Eh	δ34S (sulfate)
Depth	1.00	-0.89	-0.54	-0.81	0.27	-0.03	-0.84	0.53
Temperature	-0.89	1.00	0.29	0.65	-0.39	-0.27	0.53	-0.21
DO	-0.54	0.29	1.00	0.87	0.34	0.60	0.71	-0.40
pH	-0.81	0.65	0.87	1.00	0.04	0.35	0.79	-0.53
Turbidity	0.27	-0.39	0.34	0.04	1.00	0.74	0.02	-0.07
Chlorophyll	-0.03	-0.27	0.60	0.35	0.74	1.00	0.37	-0.49
Eh	-0.84	0.53	0.71	0.79	0.02	0.37	1.00	-0.68
34S (sulfate)	0.53	-0.21	-0.40	-0.53	-0.07	-0.49	-0.68	1.00
7-Aug-13								
CORRELATION	Depth	Temperature	DO	pH	Turbidity	Chlorophyll	Eh	δ34S (sulfate)
Depth	1.00	-0.96	0.22	-0.48	0.71	0.80	-0.91	0.03
Temperature	-0.96	1.00	-0.18	0.51	-0.75	-0.86	0.97	-0.06
DO	0.22	-0.18	1.00	0.75	0.07	-0.17	-0.06	-0.79
pH	-0.48	0.51	0.75	1.00	-0.48	-0.74	0.59	-0.70
Turbidity	0.71	-0.75	0.07	-0.48	1.00	0.92	-0.66	-0.27
Chlorophyll	0.80	-0.86	-0.17	-0.74	0.92	1.00	-0.84	0.11
Eh	-0.91	0.97	-0.06	0.59	-0.66	-0.84	1.00	-0.24
34S (sulfate)	0.03	-0.06	-0.79	-0.70	-0.27	0.11	-0.24	1.00
2-Oct-13								
CORRELATION	Depth	Temperature	DO	pH	Turbidity	Chlorophyll	Eh	δ34S (sulfate)
Depth (m)	1.00	-0.93	-0.73	-0.72	0.80	0.73	-0.64	0.63
Temp	-0.93	1.00	0.83	0.91	-0.93	-0.86	0.92	-0.81
DO	-0.73	0.83	1.00	0.96	-0.95	-0.91	0.77	-0.67
pH	-0.72	0.91	0.96	1.00	-0.98	-0.94	0.99	-0.86
Turbidity	0.80	-0.93	-0.95	-0.98	1.00	0.98	-0.99	0.92
Chlorophyll	0.73	-0.86	-0.91	-0.94	0.98	1.00	-0.94	0.98
Redox	-0.64	0.92	0.77	0.99	-0.99	-0.94	1.00	-0.86
34S (sulfate)	0.63	-0.81	-0.67	-0.86	0.92	0.98	-0.86	1.00

Table 2. Correlations by depth between field parameters and $\delta^{34}S_{sulfate}$ values in May, August, and October 2013. Values highlighted in green are strongly correlated and those in yellow are significant to a lesser extent.

PLANKTOTHRIX RUBESCENS

During seasons of thermal stratification at Crystal Lake, a layer of concentrated *P. rubescens* stratified at the metalimnion-hypolimnion boundary. *P. rubescens* cyanobacteria were collected in August and October at the depths of maximum turbidity

and chlorophyll. The *P. rubescens* collected was filamentous, contained gas vacuoles for buoyancy regulation, was reddish in color and found as an entwined mass that resulted in a layer of pink water. The cyanobacteria caused the chlorophyll and turbidity maxima at the boundary between the metalimnion and hypolimnion, where Eh was at a maximum and DO suddenly declined as other photosynthesizers respired. *P. rubescens* require minimal light, nutrient availability, and an abundance of S^{2-} from the hypolimnion for anaerobic photosynthesis (Halstvedt et al., 2007; Eq. 3). Anaerobic photosynthesis drastically affected sulfur cycling within the water column. The oscillitoroid cyanobacteria removed sulfide from the hypolimnion and added sulfate to the metalimnion as described by Chaudhary (Chaudhary et al., 2009).

The shift in trophic state observed at Crystal Lake from eutrophic to mesotrophic may have altered conditions in favor of *P. rubescens* emergence. As stated by Lampert and Sommers (1997), *P. rubescens* tend to thrive during the beginning and final stages of eutrophication. Crystal Lake was eutrophic prior to 1997 and purple sulfur bacteria (PSB) were the only microorganism present around 6 m depth until recently, where I currently observe only *P. rubescens*. Macrophytes, which were previously removed from Crystal Lake each summer, have been allowed to grow for the past few years and have likely increased lake clarity. A sewage system has been installed in the town surrounding Crystal Lake, also improving lake clarity (Collins, 1999). As in Lake Zurich, *P. rubescens* appearance in Crystal Lake seems to have followed an increase in lake transparency (Legnani et al., 2005).

Other possible reasons for the emergence of *P. rubescens* at Crystal Lake could be 1) they can survive in low light and temperatures, 2) they produce microcystins that

prevent grazing, and 3) they regulate buoyancy making them more competitive among other phytoplankton (Van den Wyngaert et al., 2011; Figueiredo, 2004).

These cyanobacteria impact the concentrations and isotopic fractionation of several sulfur compounds within Crystal Lake.

SILICA AND PHOSPHORUS

General concentration ranges for phosphorus were 0.02–1.23 mg/L PO_4^{3-}-P, 0.0037–1.21 mg/L PO_4^{3-}-P, and 0.47–1.42 mg/L PO_4^{3-}-P in May, August, and October 2013 respectively (Figure 6). Silica (SiO_2) concentrations ranges during these months were 0.077–0.55 mg/L, 0.4–3 mg/L, and 1.1–5.3 mg/L respectively. There were maxima in silica and phosphorus concentrations in the hypolimnion.

Weathering was the most likely cause of the increase in silica and phosphorus flux into the surface waters in October. Phytoplankton in the epilimnion and metalimnion used silica and phosphorus during photosynthesis. Minima in silica and phosphorus concentrations occurred in these layers of the water column. Phosphorus concentrations were lowest in August during the algae growing season. Diatom blooms occurred during times of mixing, as they were susceptible to sinking due to the weight of their frustules. This explains the low concentrations of silica in the epilimnion in the spring and fall, and the increase in concentrations in August. They could counteract this weight imbalance during these times by adding an influx of light-weight ions into their vacuoles to help slow the sinking process (Miklasz and Denny, 2010). During times of stratification they were also subjected to predation by zooplankton (Sorvari, 2001). Both phosphorus and silica concentrations increased in the metalimnion, despite the substantial *P. rubescens* in August and October. The decay of phytoplankton in the hypolimnion released nutrients,

such as silica and phosphorus, into the water column. These concentrations increased over the summer months due to increased remineralization.

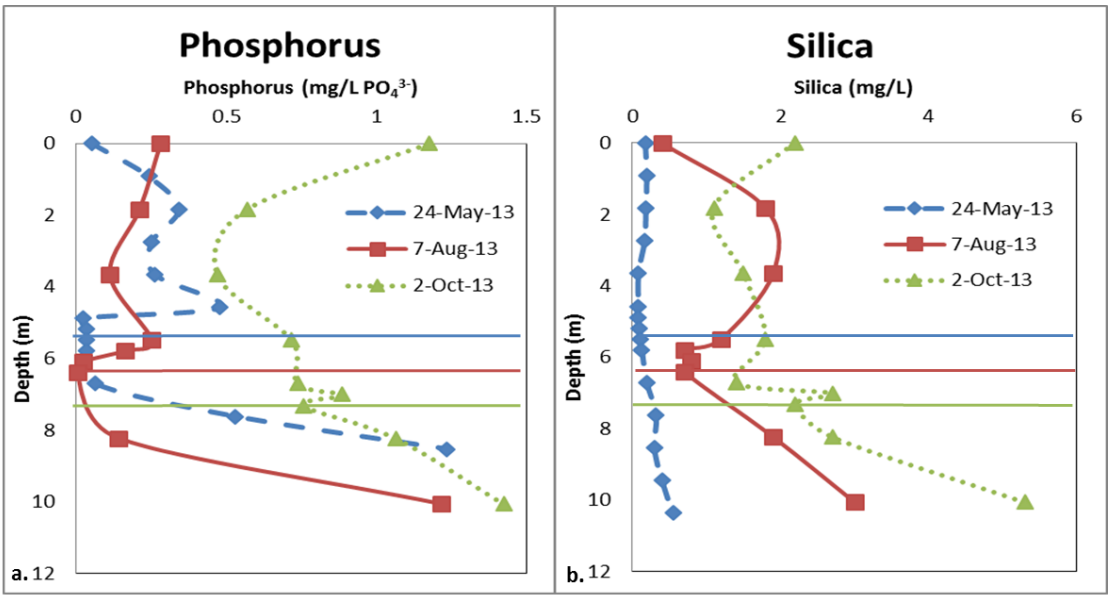

Figure 6. a. Phosphorus concentrations in May, August, and October. b. Silica concentrations in May, August, and October.

SULFATE AND SULFIDE

The biogeochemistry of Crystal Lake is controlled by thermal stratification, photosynthesis and the decomposition of organic matter. Sulfur geochemistry is an important component of these processes (Figure 7 a and b). Silica and phosphorus concentrations increased in the hypolimnion as sulfate concentrations declined during the summer stratification period (Figure 6). Sulfide concentrations increased from a minimum of 0.02 mg/L in May to a maximum of approximately 13 mg/L in October. In May, the shallowest depth that sulfide was detected was 10.4 m and below, while in

August it was measurable at 6.4 m and below and October below 7 m, with the detection range being 0.01–11.25 mg/l. The concentration of 13 mg/l in October was calculated based on the trend of sulfide in the hypolimnion. In May sulfate concentrations were high throughout the water column, and little to no sulfide was present. However, in August and October, sulfate concentrations remained relatively constant from the surface down to their respective metalimnion-hypolimnion boundaries, where a sulfate maximum existed. Sulfate concentrations decreased from the metalimnion-hypolimnion boundary to the benthos.

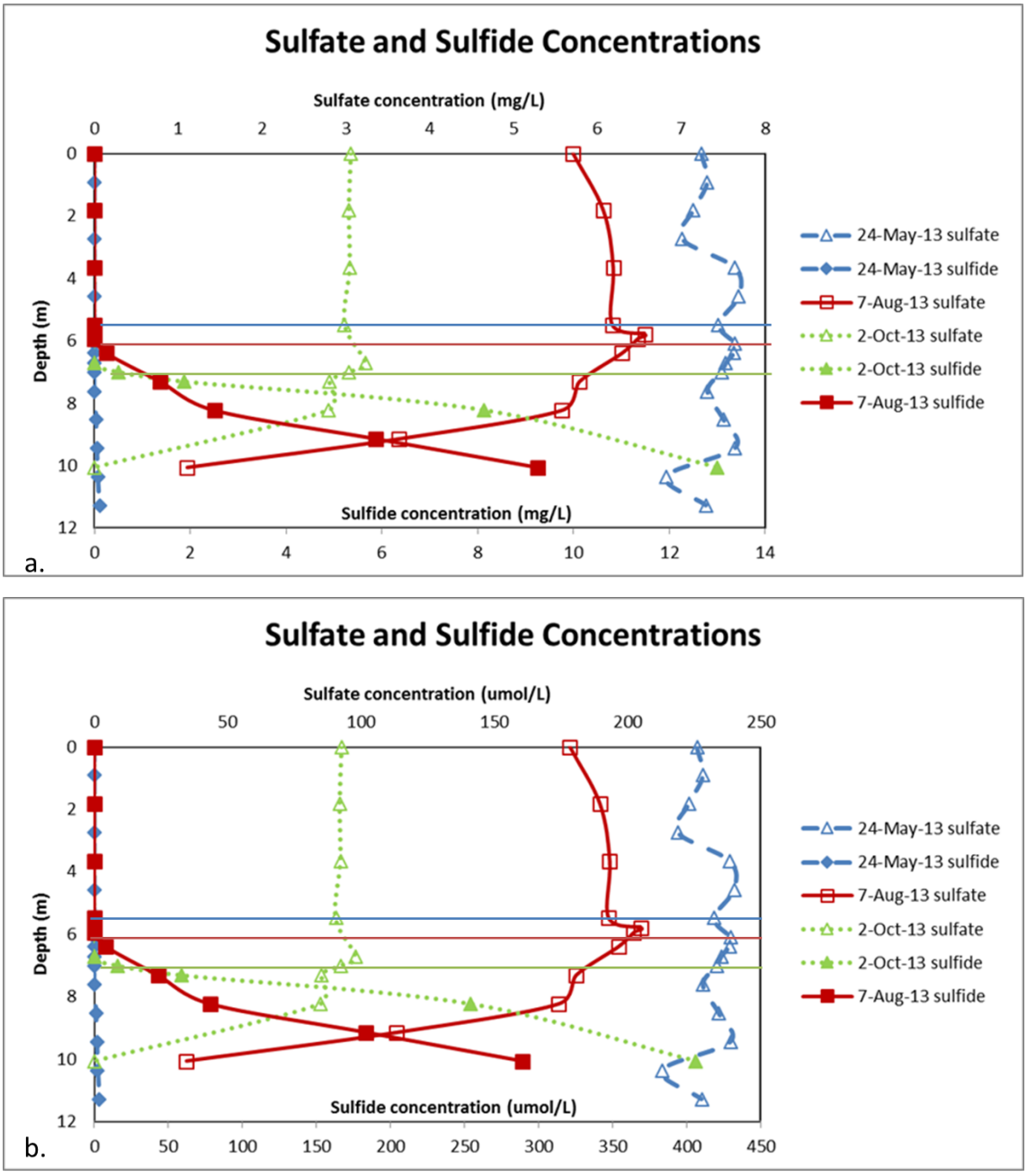

Figure 7. (a). Diagram showing observed concentrations of sulfate and sulfide in mg/L by depth on May 24, August 7, and October 2, 2013. (b). Diagram showing observed concentrations of sulfate and sulfide in µmol/L.

Presence of DO throughout the water column in May, due to the recent spring turnover, likely was the reason for the absence of sulfide and vertically constant sulfate concentrations at the beginning of the summer stratification period (Figure 4). An inverse

relationship between sulfate and sulfide in the hypolimnion suggested that, as sulfide increased with depth, sulfate decreased (Figure 8). The reason for the mirror image tendency, shown in Figure 7, is that sulfate was reduced to sulfide in this region of the lake by sulfate-reducing organisms under anoxic conditions. The redox profile and lack of DO support this conclusion.

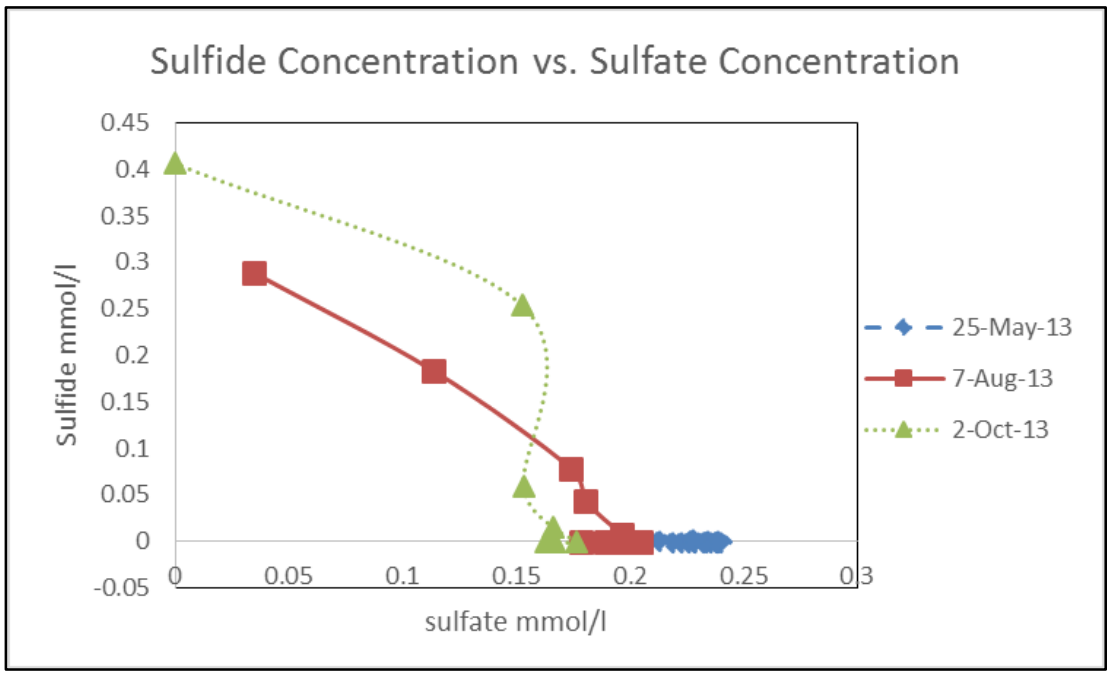

Figure 8. Sulfide vs sulfate concentrations in mmol/l in the hypolimnion. In August and October, as Sulfate decreases, sulfide increases.

If the sulfate was being reduced to sulfide, and it was the only source of the sulfide present, the sulfide + sulfate concentration in mmol/L should have remained constant throughout the water column. Sulfide + sulfate values were relatively constant with depth in May because of the recent spring turnover, allowing for sulfate to mix throughout the column, with an absence of sulfide in the hypolimnion. From May to October, the concentration of sulfide + sulfate increased in the hypolimnion and decreased in the epilimnion and metalimnion (Figure 9). Sulfate uptake by phytoplankton in the epilimnion and metalimnion was partly responsible for the decrease

in sulfide + sulfate concentration over time. As dead organisms sink to the hypolimnion, they decay and release sulfide into the anoxic water column. Sulfide could also be produced in the hypolimnion by the bottom sediments.

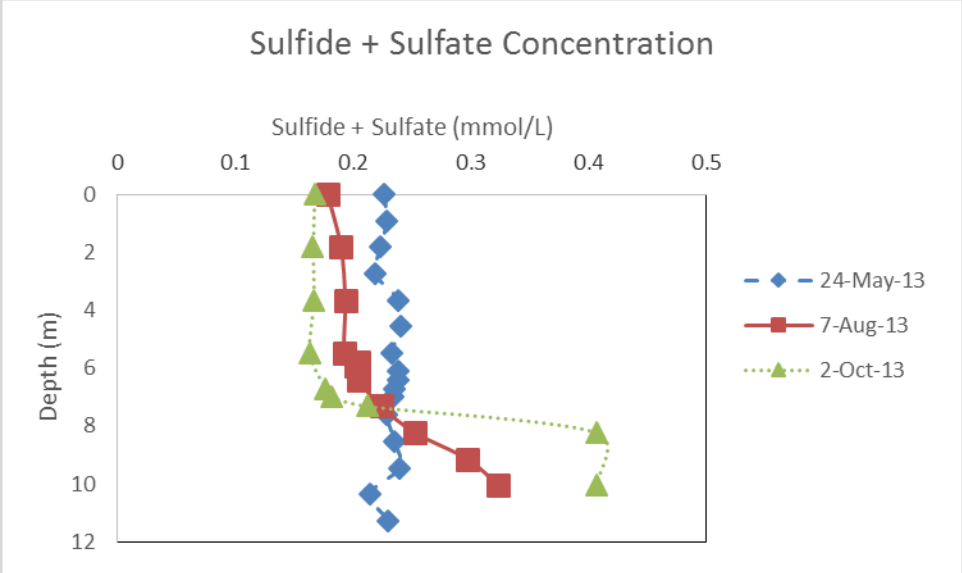

Figure 9. Sulfide + sulfate concentrations throughout the water column in May, August, and October.

Sulfate concentrations in Crystal Lake decreased dramatically from 1998-2013 (Figure 10). This may have been due, in part, to the Clean Air Act of 1970 and amendments in 1990. Power plants have installed scrubbers, and emitted approximately 50% less SO_2 into the atmosphere (epa.gov, 2009). Less SO_4^{2-} has been deposited in the epilimnion as acid rain into freshwater lakes (Jedrysek, 2005). Higher secchi disk depth measurements, and lower sulfate concentrations at Crystal Lake indicate increasing water clarity over time.

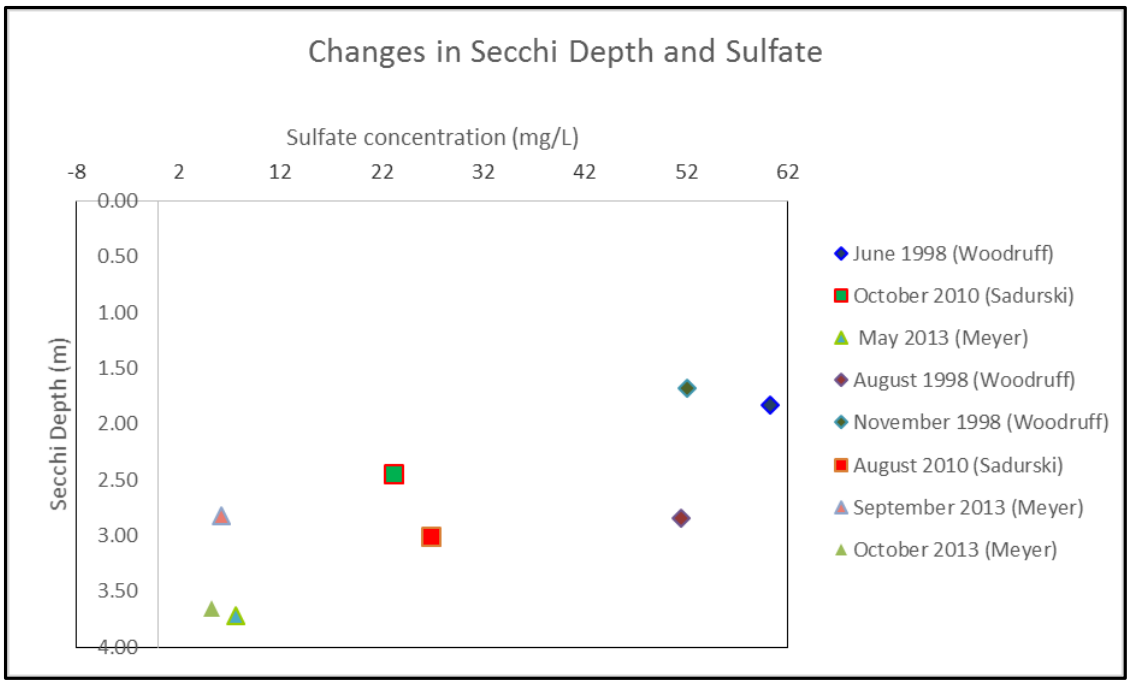

Figure 10. Changes in secchi disk depth measurements of water clarity at Crystal Lake collected in 1998, 2010, and 2013 and differences in epilimnion sulfate concentrations in the months of May-June, August-September, and October-November. (Woodruff, 1999; Sadurski, 2012).

SULFUR ISOTOPES

SULFATE AND SULFIDE

Stable isotope analysis of sulfur compounds, along with concentration measurements, allow for examination of transformations of sulfur (Jedrysek, 2005). Sulfate concentration and $\delta^{34}S_{sulfate}$ values were relatively constant in the epilimnion and metalimnion in August and October (Figure 11). May samples were collected right after spring turnover, therefore mixing and temperature fluctuations could have created a less-pronounced sulfate concentration profile. Sulfate concentrations decreased over time while $\delta^{34}S_{sulfate}$ values increased in the epilimnion from an average of 1.67 ‰ to 2.16 ‰. Small sulfate concentration maxima were observed at the boundary between the metalimnion and hypolimnion during each month measured. The maximum value

observed in August was also coupled with a $\delta^{34}S_{sulfate}$ minimum. This minimum was followed by a large increase in $\delta^{34}S_{sulfate}$ values below the boundary. An increase in $\delta^{34}S_{sulfate}$ in the hypolimnion also occurred in October. May $\delta^{34}S_{sulfate}$ values were relatively constant except in the lower hypolimnion. The sulfate maximum was at the layer of *P. rubescens* in August and October (Figure 11).

The sulfate that was produced by anaerobic photosynthesis came from H_2S (Eq. 3). When H_2S is oxidized to SO_4^{2-}, the isotopically lighter ^{32}S would be preferentially oxidized leading to a $\delta^{34}S_{sulfate}$ minimum (Garlick et al., 1977). This was observed in August only. The distribution of sulfate concentrations in May were not fully developed due to the recent spring turnover. Another potential reason for a lack of development in sulfate concentrations in the lower metalimnion in May is that the *P. rubescens* layer had not fully formed at this time. There may have been insufficient sampling around the *P. rubescens* layer in October that obscured observation of a $\delta^{34}S_{sulfate}$ minimum. A large increase in $\delta^{34}S_{sulfate}$ was observed in the hypolimnion in May, August and October due to the preferential reduction of isotopically heavier sulfate to sulfide and hence enriched ^{34}S in the residual sulfate. Sufficient quantity of sulfate for isotopic analysis was not available in August and October below 7 m, which accounts for the lack of data.

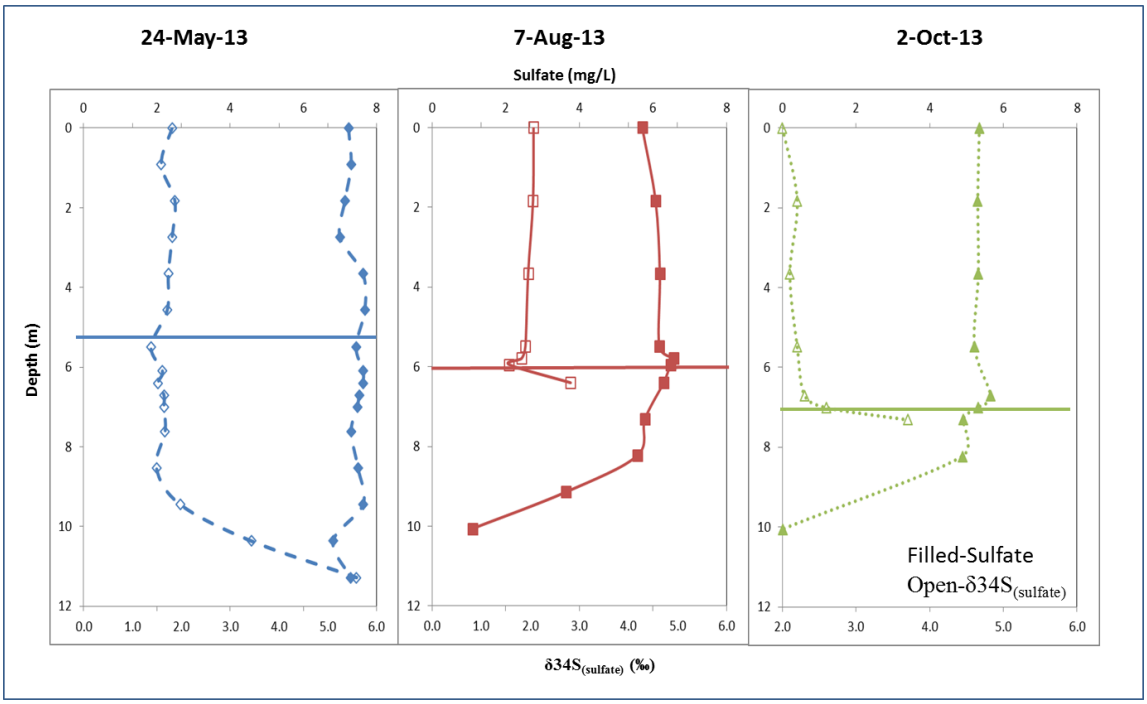

Figure 11. $\delta^{34}S_{(sulfate)}$ values and sulfate concentration by depth in May, August and October. $\delta^{34}S_{(sulfate)}$ values show a minimum at the *P. rubescens* layer (marked with a line) in August at the metalimnion-hypolimnion boundary due to oxidation of sulfide to sulfate by microbial mediation. As sulfate concentration begins to decline in the hypolimnion due to reduction to sulfide, $\delta^{34}S_{(sulfate)}$ increases.

As sulfide concentrations increased with depth in the hypolimnion, $\delta^{34}S_{sulfide}$ values also increased (Figure 12). $\delta^{34}S_{sulfide}$ values increased with depth and over time. Samples could be taken at higher depths over time due to an increase in sulfide concentrations. This pattern is due to Rayleigh fractionation and will be described next.

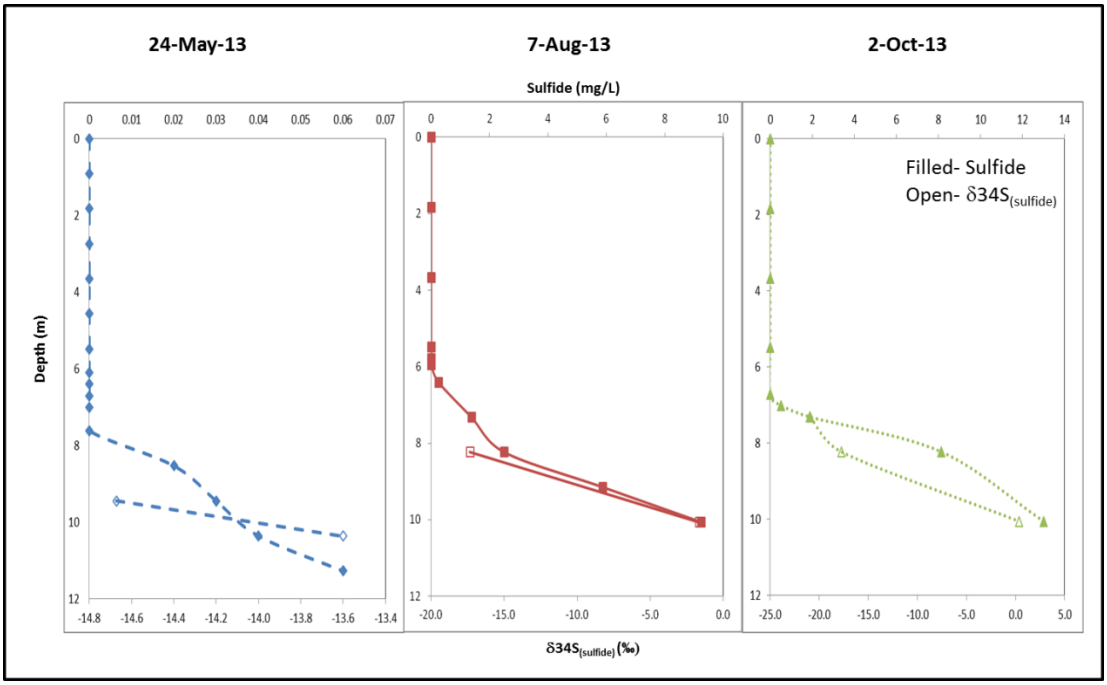

Figure 12. Sulfide concentration and $\delta^{34}S_{(sulfide)}$ composition in May, August, and October showing that as sulfide concentration increases, isotopic concentrations also increases due to Rayleigh fractionation.

Figure 13 shows the correlation between $\delta^{34}S$ of sulfate and sulfide; as sulfate was reduced to sulfide, the isotopic composition of the residual sulfate in the water became heavier. As the sulfate isotopic composition became heavier, so did the sulfide isotopic composition. This is due to Rayleigh fractionation (Eq. 7).

$$\frac{\delta+1000}{\delta_0+1000} = f^{\propto-1} \qquad \text{(Eq. 7)}$$

Where:

δ = Final $\delta^{34}S_{sulfate.}$

δ_0 = Initial $\delta^{34}S_{sulfate}$.

f = Fraction of remaining sulfate concentration.

And

α = Fractionation factor = $\frac{R_{S^{2-}}}{R_{SO_4^{2-}}}$

The fraction of remaining sulfate concentration was calculated with equation 8.

$$\frac{(SO_4^{2-})}{(SO_4^{2-})_0} = f_{a/b} \qquad \text{(Eq. 8)}$$

Where:

f = Fraction of remaining sulfate.

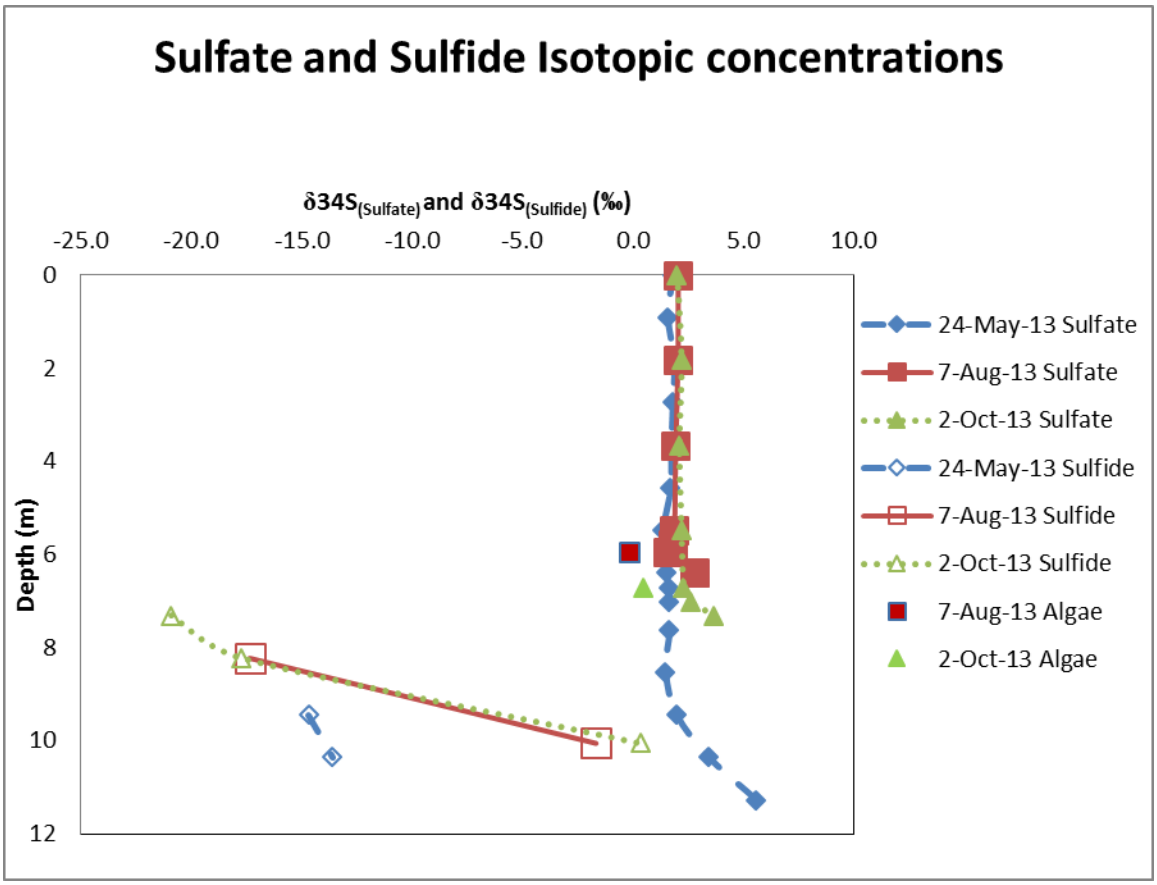

Figure 13. Diagram showing the correlation between $\delta^{34}S$ of sulfate and sulfide throughout the season due to Rayleigh fractionation and *P. rubescens* sulfur isotopic concentrations.

Figure 14 (a and b) shows the isotopic fractionation that occurred in August 2013, offset by α which was estimated to be approximately 1.024. Thode (1991) found that reduction of sulfate to sulfide produces α values around 1.024, which corresponded to the findings of the present study. The α values were estimated by starting with the 1.024 Thode found to be true, then trying other values above and below 1.024, to determine which curve more closely resembled the $\delta^{34}S_{sulfate}$ curve. The *f* values presented in figure 15 were calculated with equation 8 using sulfate concentration in they hypolimnion, and $^{34}S_{sulfide}$ values were calculated with equation 9, using the estimated α values.

$$\alpha_{12} = \frac{\delta_1 + 1000}{\delta_2 + 1000} \quad \text{(Eq. 9)}$$

Where:

α_{12} = Fractionation factor.

$\delta_1 = \delta^{34}S_{sulfate}$.

And

$\delta_2 = \delta^{34}S_{sulfide}$.

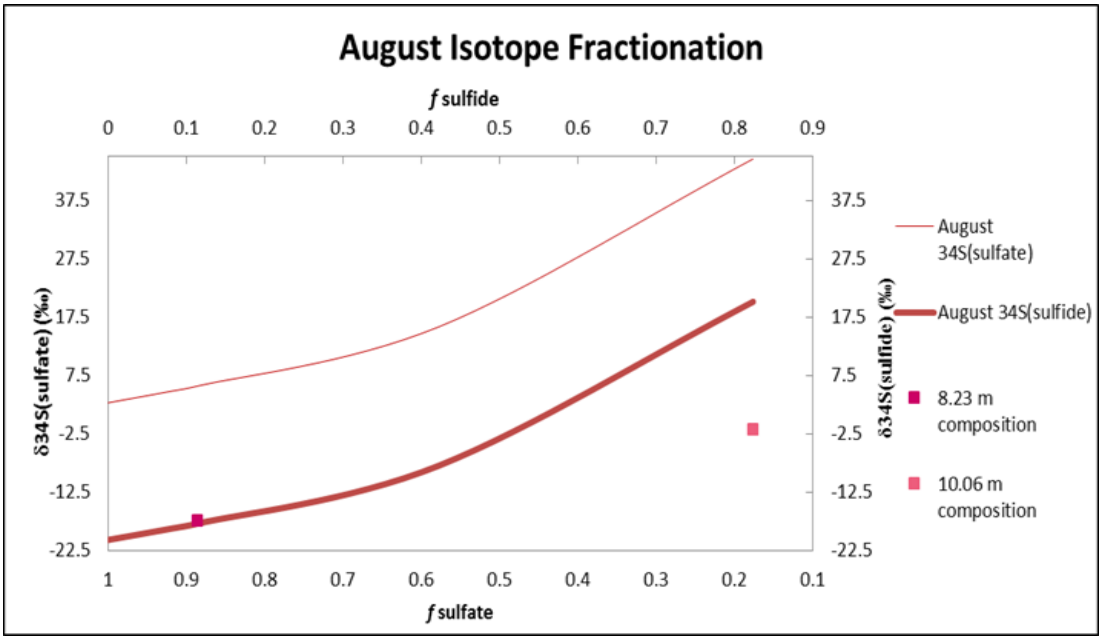

Figure 14 (a). Diagram showing the calculated amount of isotopic fractionation that occurred in August from sulfate to sulfide using α value of 1.024. Measured sulfide isotopic ratios are marked at 8.23 m depth and 10.06 m depth.

Sulfate concentration depleted as it was reduced to sulfide in the hypolimnion, increasing the heavier isotope of sulfate. As this occurred, isotopically heavier sulfide occurred due to equation 9 (Figure 15). We see this increase in measured sulfide isotope values, but the values were lower than expected at 10.06 m depth. Calculations, using equation 9 and estimated α values, show that sulfide isotope values were approximately 20 ‰ lower in August than they would be if this was the only process affecting the values (Table 3). Measurements from 8.23 m depth were fairly consistent, within 0.5 ‰, with calculated values, but measurements at 10 m depth varied significantly from the calculated values.

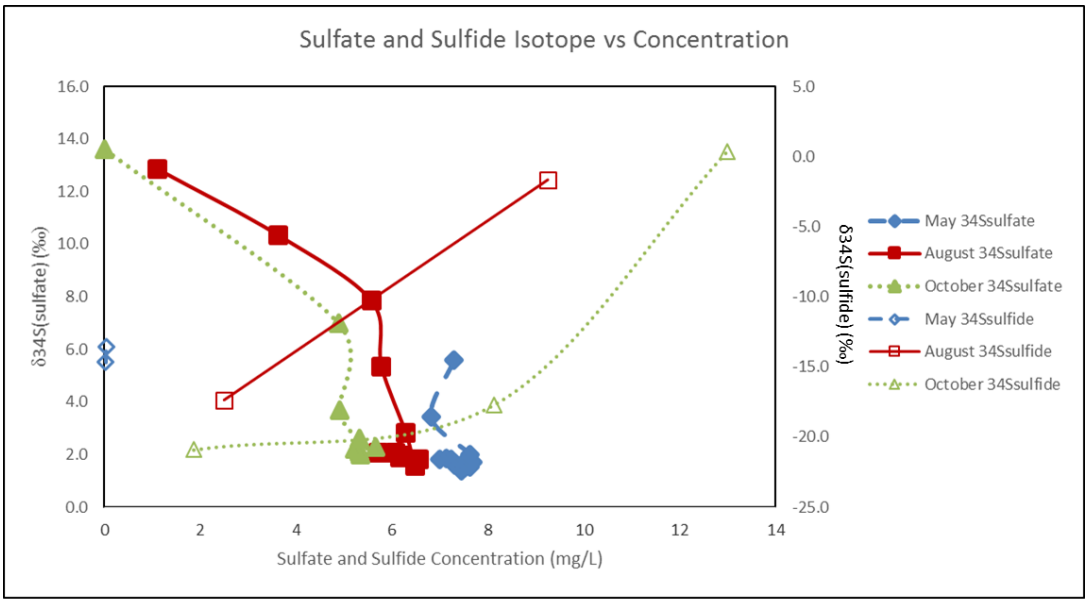

Figure 15. Sulfate and sulfide concentrations vs. isotopic compositions within Crystal Lake in May, August, and October.

August 2013 $\delta^{34}S$(sulfide)			
Calculated		Measured	
Depth (m)	Isotopic Value (‰)	Depth (m)	Isotopic Value (‰)
6.4	-20.7		
7.31	-18.7		
8.23	-17.9	8.23	-17.4
9.14	-8.0		
10.06	20.1	10.06	-1.7

Table 3. Calculated and measured $\delta^{34}S$sulfide compositions in August, 2013.

This offset can most likely be attributed to the addition of hydrogen sulfide into the hypolimnion due to the decay of dead organisms that have sunk to the bottom of the hypolimnion by sulfate reducing bacteria and microbial putrefaction of proteinaceous material in bottom sediments (Dunnette, 1985). Sulfate isotopic composition could not be measured in the hypolimnion in August and October due to lack of sulfate for analysis, therefore calculations were performed based on the trend of analyzed concentrations. This could be another source of the offset in sulfide isotopic composition calculations and

measured values, especially at 10.06 m. May fractionation trends could not be observed due to little sulfide and high sulfate content within the water column

P. RUBESCENS

P. rubescens were analyzed for sulfur $^{34}S/^{32}S$ ratio as well. August and October were the only months that sufficient quantity of sample could be attained for isotopic analysis. Sulfur isotopic compositions were fairly similar each month, but varied between -0.15 and 0.48 ‰. These values are marked at the depth of *P. rubescens* in Figure 13. No published results of *P. rubescens* composition could be found to compare to. However, α values based on those two samples are 0.983 for August and 0.979 for October (Eq. 10).

$$\alpha_{12} = \frac{\delta_1 + 1000}{\delta_2 + 1000} \qquad \text{(Eq. 10)}$$

Where:

α_{12} = Fractionation factor.

$\delta_1 = \delta^{34}S_{sulfide}$.

And

$\delta_2 = \delta^{34}S_{P.\ rubescens}$.

Judging by the minimum in $\delta^{34}S_{sulfate}$ and maximum in sulfate concentrations shown in August in figure 11, sulfide oxidation to elemental sulfur, then to sulfate occured due to microbial mediation by *P. rubescens* at the metalimnion-hypolimnion boundary. Because of this determination, it is reasonable to assume that the ^{34}S analyzed in the *P. rubescens* came from S^{2-} as opposed to SO_4^{2-}. The α calculations were performed between the *P. rubescens* and S^{2-} due to this observation. Complications exist due to the oxidation of S^0

in *P. rubescens* to SO_4^{2-} not being included in the calculations. Also, the Pearson-Plummer-Wigley equation could handle this one-in-one-out situation, but the Rayleigh fractionation equation can only deal with a one-out situation (Wigley, Plummer and Pearson, 1978). The α could affect ^{34}S in the water column due to in situ fractionation occurring in the hypolimnion. It could also affect ^{34}S due to dead *P. rubescens* sinking to the bottom of the hypolimnion. As the dead phytoplankton decay, they release sulfide and other nutrients into the water column. Bacterial sulfate reduction has been shown to produce $\alpha_{SO4\text{-}H2S}$ around 1.077 (Rudnicki, 2001). Other types of cyanobacteria α values could not be acquired. This discrepancy could be due to *P. rubescens* sulfide oxidation as opposed to sulfate reduction. The $\delta^{34}S$ of *P. rubescens* are slightly lower than that of the SO_4^{2-}, and due to the fact that the sulfate isotopic values are at a minimum at this depth, the original hypothesis, that the *P. rubescens* values are lower due to the S^0 within the cells originating from H_2S, seems very likely. As H_2S is isotopically lighter that SO_4^{2-}, this seems to be a valid hypothesis.

Mass balance was performed to determine if the addition of sulfate concentrations due to sulfide oxidation by *P. rubescens*, with the lighter ^{34}S composition of the cyanobacteria, could have resulted in the final ^{34}S value of the aqueous sulfate at the metalimnion-hypolimnion boundary (Eq. 11).

$$(c_1 * m_1) + (c_2 * m_2) = (c_3 * m_3) \quad \text{(Eq. 11)}$$

Where:

c_1 = Amount of sulfate concentration contributed from *P. rubescens*.

m_1 = Unknown: $^{34}S_{P.rubescens}$

c_2 = Average concentration of sulfate in the epilimnion-metalimnion.

m_2 = $^{34}S_{sulfate}$ just above the *P. rubescens* layer.

c_3 = Sulfate concentration at the metalimnion-hypolimnion boundary.

m_3 = $^{34}S_{sulfate}$ at the metalimnion-hypolimnion boundary.

The amount of sulfate contributed from *P. rubescens* was calculated by subtracting the average concentration in the epilimnion-metalimnion from the maximum concentration at the *P. rubescens* layer. The resulting calculation of $^{34}S_{P.rubescens}$ was -2.74 ‰ in August whereas the analytical results were -0.15 ‰. There are several possibilities for the difference in calculated and analytical values observed. One such reason could be that the *P. rubescens* analyzed were not an instant product, but a cumulative mass. Another possibility is that the sulfur inside the *P. rubescens* has a different ^{34}S than that of sulfate coming from the oxidation of elemental sulfur, i.e. isotopic fractionation occurring during the oxidation of S^0 of *P. rubescens* to sulfate in the water column. It is possible that there is a preferential oxidation of the lighter ^{32}S over ^{34}S in this situation. Utilizing equation 10, an α value could be calculated using the calculated $^{34}S_{P.rubescens}$ value of -2.74. The resulting α value was 0.985, merely 0.002 away from the α calculated from the analytical $^{34}S_{P.rubescens}$.

CORRELATIONS BETWEEN FIELD PARAMETERS AND $^{34}S_{sulfate}$

The $^{34}S_{sulfate}$ was weakly positively correlated with depth and negatively correlated with pH and redox in May (Table 2). The $^{34}S_{sulfate}$ was negatively correlated with both DO and pH during August. The $^{34}S_{sulfate}$ was found to be strongly correlated with temperature, pH, turbidity, chlorophyll, and redox in October. There was a negative sulfate isotope correlation with temp, DO, pH and redox during this period. As they

decrease, isotope concentration increases. Turbidity, chlorophyll, and depth increase at similar rates as isotopic concentration increases.

The $^{34}S_{sulfate}$ found a positive correlation with depth as concentrations increase with depth due to the reduction of sulfate to sulfide in the hypolimnion. The pH and redox decrease in the hypolimnion due to respiration of *P. rubescens* while $^{34}S_{sulfate}$ concentrations increase. As redox becomes negative in the hypolimnion due to absence of DO, sulfate is reduced to sulfide. This is part of the reason for the negative correlation between DO and $^{34}S_{sulfate}$ concentration. The negative correlations with sulfate isotopic composition is also partially attributed to the preferential uptake of the lighter ^{32}S over ^{34}S, increasing the $^{34}S/^{32}S$ ratio. High turbidity measurements occur as more primary production takes place. Primary production is also the reason for the higher concentrations of DO, high pH values, and high chlorophyll concentrations.

IV. CONCLUSION

It was observed that temperature, photosynthesis, the decay of organic matter, and sulfur processes all played a role in governing the biogeochemistry of the lake. Results of field parameters measured were as expected for a dimictic lake during this period. Thermal stratification occurred during the warmer months due to the high depth to surface area ratio, affecting many other processes observed. The pH and DO maxima in the metalimnion were caused by photosynthesis reactions consuming CO_2 and releasing DO, and low DO values in the hypolimnion were due to the decay of organic matter. Thermal stratification and the decay of organic matter in the hypolimnion caused the negative Eh values in May and August. Chlorophyll and turbidity maxima at the metalimnion-hypolimnion boundary were also caused by algae and photosynthesis. Silica and phosphorus concentrations were at a minimum in the epilimnion and metalimnion due to uptake by algae during photosynthesis, and increased in the hypolimnion due to the decay of organic matter.

Spring turnover in April resulted in reduced thermal stratification and a mixing of DO and other nutrients throughout the water column. Sulfide produced by bottom sediments was immediately oxidized to sulfate during spring turnover when oxygen was still present. August and October sulfate maxima occurred at the metalimnion-hypolimnion boundary due to anaerobic photosynthesis by *P. rubescens* oxidizing sulfide to sulfate. In

the anaerobic hypolimnion, sulfate values decline due to reduction to sulfide, which increased with depth in the hypolimnion as sulfate was reduced and respiration occured. Sulfate concentrations have decreased over time, from 1998 to present, and even month to month, due to the Clean Air Act of 1970 and the amendments of 1990.

Identifying a layer of *P. rubescens* at the metalimnion-hypolimnion boundary was extremely helpful in predicting what processes could be taking place within the water column as the algae are possible anaerobic photosynthesizers. Purple sulfur bacteria (PSB) were found at the metalimnion-hypolimnion boundary in the 2012 study by Stephen Sadurski. The transition from PSB to *P. rubescens* was due to an increase in lake clarity.

Analysis of different sulfur species was mandatory to determine the fractionation between the different sulfur elements in the water column. The process of reduction of sulfate to sulfide also made the residual SO_4^{2-} isotopically heavier. A minimum in $\delta^{34}S_{sulfate}$ composition at the *P. rubescens* layer occurred due to oxidation of sulfide to sulfate through microbial mediation. Production of sulfate during this process derives from sulfide, which is isotopically lighter than SO_4^{2-}. Sulfate isotopic composition increased in the hypolimnion where reduction occured and sulfate concentration decreased. Isotopic measurements of sulfide were found to also increase in the hypolimnion as sulfate isotopic composition increased due to Rayleigh fractionation. The sulfur isotopic composition of *P. rubescens* were slightly lower than sulfate isotopic composition measured from the same depth. This is most likely resulting from the source of sulfur within the cells. Oxidation of H_2S to S^0 would produce an isotopically lighter abundance ratio within the cell as 32S is preferentially oxidized during this process.

Future studies are needed to determine if *P. rubescens* can switch between aerobic and anaerobic photosynthesis. This would help in determining whether the sulfur compounds and isotopic fractionation are being effected by the algae, or if some other process is dominant. Future studies should also incorporate sulfate concentration measurements and isotopic analysis of sulfate in rainwater. This would give researchers an idea of how much the industrial facilities in the region contribute to the source of sulfate in Crystal Lake. Another possible laboratory study that could be performed based on this research would be to determine what exactly causes the difference between $^{34}S_{P. rubescens}$ values analyzed and calculated.

V. APPENDICES

APPENDIX A

STATISTICAL ANALYSIS

CORRELATION MATRICES.

- Correlations with values that have an absolute value ≥ 0.7 are shown in parenthesis.
- Correlations with values between 0.5 and 0.7 are displayed with a (*).
- Strongly significant values are marked with a (*) and placed in parenthesis.
- Correlations show that as depth increases, temperature, dissolved oxygen, pH and redox decrease.
- As depth increases, turbidity, chlorophyll and $\delta^{34}S_{sulfate}$ also increase.

24-May-13								
CORRELATION	Depth	Temperature	DO	pH	Turbidity	Chlorophyll	Eh	δ^{34}S (sulfate)
Depth	1.00	(-0.89)	*-0.54	(-0.81)	0.27	-0.03	(-0.84)	*0.53
Temperature	(-0.89)	1.00	0.29	*0.65	-0.39	-0.27	*0.53	-0.21
DO	*-0.54	0.29	1.00	(-0.87)	0.34	*0.60	(-0.71)	-0.40
pH	(-0.81)	*0.65	(-0.87)	1.00	0.04	0.35	(-0.79)	*-0.53
Turbidity	0.27	-0.39	0.34	0.04	1.00	(-0.74)	0.02	-0.07
Chlorophyll	-0.03	-0.27	*0.60	0.35	(-0.74)	1.00	0.37	-0.49
Eh	(-0.84)	*0.53	(-0.71)	(-0.79)	0.02	0.37	1.00	*-0.68
δ^{34}S (sulfate)	*0.53	-0.21	-0.40	*-0.53	-0.07	-0.49	*-0.68	1.00

7-Aug-13								
CORRELATION	Depth	Temperature	DO	pH	Turbidity	Chlorophyll	Eh	δ^{34}S (sulfate)
Depth	1.00	*(-0.96)	0.22	-0.48	(-0.71)	(-0.80)	*(-0.91)	0.03
Temperature	*(-0.96)	1.00	-0.18	*0.51	(-0.75)	(-0.86)	*(0.97)	-0.06
DO	0.22	-0.18	1.00	(-0.75)	0.07	-0.17	-0.06	(-0.79)
pH	-0.48	*0.51	(-0.75)	1.00	-0.48	(-0.74)	*0.59	(-0.70)
Turbidity	(-0.71)	(-0.75)	0.07	-0.48	1.00	*(0.92)	*-0.66	-0.27
Chlorophyll	(-0.80)	(-0.86)	-0.17	(-0.74)	*(0.92)	1.00	(-0.84)	0.11
Eh	*(-0.91)	*(0.97)	-0.06	*0.59	*-0.66	(-0.84)	1.00	-0.24
δ^{34}S (sulfate)	0.03	-0.06	(-0.79)	(-0.70)	-0.27	0.11	-0.24	1.00

2-Oct-13								
CORRELATION	Depth	Temperature	DO	pH	Turbidity	Chlorophyll	Eh	δ^{34}S (sulfate)
Depth	1.00	*(-0.93)	(-0.73)	(-0.72)	(-0.80)	(-0.73)	*-0.64	*0.63
Temperature	*(-0.93)	1.00	(-0.83)	*(0.91)	*(-0.93)	(-0.86)	*(0.92)	(-0.81)
DO	(-0.73)	(-0.83)	1.00	*(0.96)	*(-0.95)	*(-0.91)	(-0.77)	*-0.67
pH	(-0.72)	*(0.91)	*(0.96)	1.00	*(-0.98)	*(-0.94)	*(0.99)	(-0.86)
Turbidity	(-0.80)	*(-0.93)	*(-0.95)	*(-0.98)	1.00	*(0.98)	*(-0.99)	*(0.92)
Chlorophyll	(-0.73)	(-0.86)	*(-0.91)	*(-0.94)	*(0.98)	1.00	*(-0.94)	*(0.98)
Eh	*-0.64	*(0.92)	(-0.77)	*(0.99)	*(-0.99)	*(-0.94)	1.00	(-0.86)
δ^{34}S (sulfate)	*0.63	(-0.81)	*-0.67	(-0.86)	*(0.92)	*(0.98)	(-0.86)	1.00

APPENDIX B

DETAILED ANALYTICAL METHODS

ANALYSIS OF MAJOR ANIONS USING ION CHROMATOGRAPHY

Field samples were acquired and filtered in the lab with 0.2 µm filter membranes and a vacuum pump prior to analysis. Anion samples were kept at 1.6–4.4 ºC until analysis. Directly before analysis, samples were warmed to room temperature and poured into Dionex vials for analysis with a Dionex ICS-1500. Calculations were performed to determine the anion concentrations within the samples using known standard concentrations.

ANALYSIS OF PHOSPHORUS USING SPECTROPHOTOMETRY

Samples were analyzed using a Hach Spectrophotometer (DR 4000), programmed with the number 3036 setting and using a wavelength of 890 nm. 5 mL of the samples were poured into "Total and Acid Hydrolyzable Test Vials" and one potassium persulfate powder pillow for phosphonate was added to each vial. The vials were capped and shaken to mix all contents. Each vial was heated in a COD reactor for 30 minutes, then cooled to room temperature. 2 mL of 1.54 N sodium hydroxide standard solution was mixed into each vial. Fingerprints were removed from the outside of the vials with a damp, and then a dry towel. The vials were sequentially placed in the Hach DR 4000 and zeroed with a blank sample. The contents of one PhosVer 3 Powder Pillow were added to each vial, which was then capped and shaken to mix for 10-15 seconds. Reaction was allowed to ensue for 2 minutes. The vials were again placed in the Hach, the light shield closed, and PO_4^{3-} mg/L results were displayed.

ANALYSIS OF ALKALINITY USING SPECTROPHOTOMETRY

A modified Sarazin's Method was performed to determine the alkalinity of each sample. A 0.1 M $NaHCO_3$ stock solution was diluted to make standard solutions ranging from 1 mM to 8 mM. A color reagent was prepared from 25 mL of 0.15 M formic acid and 25 mL of 500 mg/L Bromophenol-Blue. This solution was diluted with distilled water in a 250 mL Erlenmeyer flask.5 mL of this reagent was added to 5 mL of sample water or standard solution, and mixed thoroughly to outgas carbon dioxide. Absorbance was measured for each sample and standard at a wavelength of 590 nm using a Hach Spectrophotometer. The Hach was blanked with distilled water when measuring the absorbance of standards, and with filtered sample water when measuring water samples. Standard absorbance measurements were fit with a 2^{nd} order polynomial to find the standard curve. Concentrations of the water samples could then be calculated using the equation from the curve.

ANALYSIS OF SULFIDE USING THE HACH FIELD KIT

Sulfide samples were taken from the hypolimnion and tested within one hour of collection. Samples were pumped directly from the hypolimnion to 3 L sample bottles which were overflowed to prevent oxygen bubbles from getting trapped in the bottle between collection and analysis. Samples were not filtered prior to analysis. 25 mL of sample was poured into two glass tubes, in which Reagent 1 was then added. The solution was mixed for 30 seconds, then Reagent 2 was added. Mixture

again occurred for 30 seconds, then the color of the solution was compared to the concentration colorimeter of the Hach Field Kit.

ANALYSIS OF AMMONIA WITH THE HACH FIELD KIT

Samples were taken from the hypolimnion to measure ammonia concentrations, and were not filtered prior to analysis. Two glass tubes were filled with 5 mL of sample water to be tested. Three drops of Nessler Reagent were added to one of the tubes, which was then swirled to mix. Color development took 1-5 minutes. If a yellow color developed, ammonia was present in the sample. The color of this solution was compared to the untreated sample in the comparator of the Hach Field Kit.

ANALYSIS OF SILICA USING SPECTROPHOTOMETRY

Silica measurements were performed within two days of collection. 0.5 mL of HCl and 1.0 mL of AM were mixed into 25 mL of sample water and allowed to react for five minutes. 1.0 mL OA was then added and mixed. The solution was then analyzed with a Hach DR 4000 at a wavelength of 410 nm. Standards of known concentrations were analyzed prior to the water samples and evaluated to find a standard curve, obtaining an R^2 value close to 0.999.

WATER SAMPLE PROCESSING FOR SULFUR ISOTOPIC COMPOSITION

Water samples designated for sulfate isotope analysis were collected in 1 L plastic bottles and refrigerated to maintain 35-40 ºC. Samples taken from the hypolimnion, where sulfide was present, were pumped directly from the desired depth to the bottle, and overflowed, to eliminate exposure to oxygen. The samples were immediately bubbled in the field with nitrogen (N_2) gas for 15-30 minutes to outgas $H_2S_{(g)}$. All samples were then taken to the lab to be filtered with a 0.22 µm filter membrane and vacuum pump. They were then acidified to pH 3-4 with dilute sulfate-free hydrochloric acid (HCl). This converted dissolved inorganic carbon (DIC) to carbonic acid (H_2CO_3) in order to eliminate carbonate (CO_3^{2-}). This was a crucial step in the process as to prevent $BaCO_{3(s)}$ co-precipitation when $BaCl_{2(aq)}$ was added. The samples were then heated for 10-15 minutes. 4-5 mL of 10% $BaCl_{2(aq)}$ was added, while stirring, and the samples were allowed to react while heating for 30 minutes. The samples were then covered and allowed to cool overnight. The samples could then be filtered to collect the $BaSO_{4(s)}$ precipitate, which was then rinsed with DI water into centrifuge tubes. The water samples were then treated again with $BaCl_2$ and heated to precipitate any remaining sulfate from the samples. The treated water was allowed to cool overnight and filtered the following day to remove any precipitate. This precipitate was then added to the designated centrifuge tube and each tube was centrifuged for approximately 10 minutes. The DI water was decanted and the $BaSO_4$ precipitate was dried in a desiccator.

Samples designated for sulfide isotopic analysis were collected in 3 L bottles. Samples were pumped directly from the desired depth to the bottles and overflowed to eliminate contact with oxygen. Samples with greater than 1 mg/L sulfide were treated in

the field with a calculated amount of 10 weight percent silver nitrate (AgNO3) to precipitate silver sulfide (Ag2S(s)). The precipitated mixture of Ag2S(s) and other compounds was filtered from the water samples in the lab. 3 weight percent ammonium hydroxide (NH4OH) was added to the precipitate to eliminate the other silver compounds and to re-suspend Co- into solution The Ag2S(s) was filtered a second time with a 0.22 μm membrane, rinsed, and dried in a desiccator. All isotope samples were sent to the University of Arizona for analysis using a mass spectrometer.

APPENDIX C

BIOGEOCHEMICAL AND ANALYTICAL DATA

CYRSTAL LAKE FIELD DATA

April 25, 2013. 12:00 P.M.

Depth (m)	Temperature (°C)	D.O. (mg/l)	Conductivity	Chlorophyll	Turbidity	pH
0.2134	14.06	14.25	557	2.6	-1.5	8.64
0.701	14.03	14.62	557	2.73	-1.5	8.48
1.615	14.18	15.02	557	4.6	-1.5	8.29
2.957	10.95	16.09	567	3.1	-1.4	8.23
3.048	9.48	18.3	567	5.7	-1.2	8.23
4.877	6.1	18.71	566	14.1	-0.6	8.37
5.365	5.6	15.35	567	41	2	7.93
5.369	5.61	13.92	567	41.6	1.6	8.04
5.7				42.1		
5.944	5.41	12.6	569	36.6	1.4	7.89
6.096	5.44	15.38	571	32	1.1	8.2
6.706	5.16	11.34	572	17.3	-0.7	7.97
7.132	5.14	13.77	573	11.1	-1	8.11
8.077	5.1	14.08	576	9.2	-1	7.9
9.601	5.06	8.87	582	6.4	-0.3	7.81
10.577	5.06	3.72	582	5.4	-0.3	7.78
11.524	5.12	0.32	594	15.2	6.2	7.64

May 1, 2013. 1:00 P.M.

Depth (m)	Temperature (ºC)	Conductivity	D.O. (mg/l)	pH	Turbidity	Chlorophyll	Redox
0	20.21	561	9.94	8.14	-2.1	1.8	101
0.341376	20.18	561	10.18	8.19	-2.1	1.2	99.7
0.70104	20.06	562	10.21	8.21	-2.1	1.7	97.8
0.978408	17.96	563	10.79	8.24	-1.9	2.7	99.7
1.210056	16.8	561	11.15	8.25	-1.9	3	100.5
1.56972	16.24	560	11.08	8.24	-1.8	2.4	100.9
1.88976	15.09	561	11.14	8.24	-1.8	2.4	102.1
2.1336	13.96	561	11.14	8.21	-1.7	3	103
2.56032	13.3	563	10.93	8.25	-1.6	3	104.4
2.846832	12.85	564	10.95	8.26	-1.6	3.5	105.5
3.090977	11.5	567	11.67	8.3	-1.3	4.2	106.6
3.39852	10.45	568	12.65	8.3	-1.3	4.3	108.5
3.767328	8.3	571	14.19	8.26	-1.3	4.3	112.4
4.087368	7.44	567	14.1	8.2	-1.3	4.4	114.3
4.23672	7.2	567	13.42	8.03	-1.2	4.9	115.6
4.517136	6.83	567	13.29	8.01	-1.1	5.1	116.4
4.876495	6.46	567	13.08	7.98	-0.9	6.7	116.8
5.162093	6.32	566	13.05	7.97	-0.8	8.6	117
5.538216	6.13	566	13.2	7.97	-0.5	11	117
5.800344	5.98	566	13.15	8.94	-0.1	12	117
6.167933	5.72	569	11.92	7.83	1.3	22.6	117.7
6.512357	5.33	570	10.61	7.74	1.8	30.5	118
6.73669	5.42	570	9.85	7.71	1.9	30.8	118.4
7.035089	5.39	571	9.57	7.69	0.9	26.7	118.8
7.363663	5.27	572	8.93	7.64	0.2	21.2	118.9
7.647127	5.19	573	7.82	7.7	-0.3	17.4	119.1
7.998257	5.17	576	6.6	7.73	-0.7	11.8	119.1
8.272882	5.16	577	5.06	7.55	-0.8	8	118.6
8.634984	5.13	579	4.03	7.52	-0.8	6.6	118.5
8.819998	5.13	580	2.66	7.53	-0.3	6.4	118.7
9.187586	5.12	581	1.37	7.46	0.6	6	117.9
9.205874	5.11	582	3.94	7.49	-0.3	5.3	4.95
9.458554	5.12	581	0.53	7.43	0.3	6	115.4
9.487814	5.11	581	0.23	7.3	-0.2	5.7	7.3
9.7536	5.1	580	0.26	7.31	-0.2	5.2	8.9
9.764268	5.12	581	0.32	7.36	2.5	6.9	111.3
10.12942	5.1	582	0.18	7.31	0.1	7.4	-0.9
10.42599	5.1	583	0.15	7.3	0.8	8.2	-51.2
10.65703	5.12	587	0.12	7.27	0.9	6.7	-138.7
11.05449	5.13	588	0.12	7.26	0.8	6.9	-159.7

May 2, 2013. 12:00 P.M.

Depth (m)	Temperature (°C)	Conductivity	DO (mg/l)	pH	Redox
0.011582	20.85	564	9.34	8.28	186.8
0.916838	18.08	560	10.69	8.34	176.4
1.837944	14.45	561	10.97	8.26	171.1
2.769108	11.94	566	11.56	8.22	168.8
3.667354	8.18	566	13.7	8.22	165
4.575353	6.3	569	14.07	8.14	164.4
5.501335	5.69	567	14.07	8.18	162.9
6.413906	5.2	573	12.8	7.86	165.7
7.331964	5.06	575	10.49	7.72	166
8.246974	4.97	579	8.06	7.59	166.1
9.156192	4.91	582	5.86	7.5	165.6
10.08461	4.91	582	4.12	7.45	147.2
10.37082	4.92	584	3.23	7.42	-166.8
11.04047	4.97	605	2.42	7.21	-241.8

May 24, 2013. 11:55 A.M.

Depth (m)	Temperature (°C)	Conductivity	DO (mg/l)	pH	Turbidity	Chlorophyll	Redox
0.0073152	21.29	547	10.08	8.27	0.9	3	41
1.0207752	21.31	548	9.75	8.37	0.8	3.1	16
1.941576	21.29	549	9.66	8.38	1.1	3.8	12.2
2.855976	16.04	557	13.07	8.39	0.9	5.1	12.5
3.7252656	11.51	556	16.88	8.4	6	8.9	14.5
4.6491144	8.34	565	15.81	8.12	1.9	8.9	20.8
5.4571392	6.67	566	13.4	7.85	2.4	6	23.6
6.1469016	5.89	570	10.94	7.66	5.9	7	24.9
6.4300608	5.8	572	9.18	7.59	4	5.4	25
6.8192904	5.59	576	4.43	7.49	3	6.2	23.1
7.0930008	5.53	577	3.19	7.46	3.3	5.8	21.2
7.6818744	5.47	577	1.71	7.46	4.3	5	19.1
8.6038944	5.37	580	0.88	7.4	4	7	-214.7
9.4942152	5.33	584	0.49	7.38	5	6.3	-236
10.442143	5.33	593	0.42	7.29	3.8	6.5	-239.5
10.923118	5.39	630	0.22	6.95	0.2	-0.3	-262.9

June 7, 2013. 2:32 P.M.

depth	Depth (m)	Temperature (°C)	Conductivity	DO (mg/L)	pH	Turbidity	Chlorophyll
0.058	0.017678	23.99	534	7.64	8.47	2.2	4.5
3.037	0.925678	23.09	534	7.95	8.48	2.4	6.1
6.086	1.855013	22.3	534	8.19	8.47	2.4	7.1
9.09	2.770632	19.42	541	10.4	8.51	3.3	9.4
12.042	3.670402	13.8	544	14.93	8.46	7.8	20
15.158	4.620158	9.37	555	14.16	8.33	9.7	16.1
18.031	5.495849	7.82	562	12.88	8.15	8.4	10.4
20.163	6.145682	6.6	564	10.48	7.93	4.2	6.4
23.089	7.037527	5.83	571	4.61	7.65	2.3	5.4
26.074	7.947355	5.58	574	1.6	7.54	8	12.6
29.063	8.858402	5.39	575	0.6	7.38	3.4	7
32.122	9.790786	5.33	580	0.43	7.37	4.2	6.9
35.188	10.7253	5.41	600	0.31	7.21	8.8	6.4
25.083	7.645298	5.66	573	0.21	7.49	14.3	20.4
24.527	7.47583	5.7	573	0.17	7.51	12.4	18.4
24.579	7.491679	5.72	572	0.22	7.45	13.9	20.6
24.664	7.517587	5.71	572	0.22	7.41	16.9	25
13.659	4.163263	11.36	544	10.63	8.48	14.1	27.1

June 24, 2013. 11:00 A.M.

Depth (m)	Temperature (°C)	Conductivity	DO (mg/l)	pH	Turbidity	Chlorophyll	Redox
0	28.33	539	8.93	8.19	0.6	2.9	53.5
0.9144	27.62	538	7.96	8.3	0.7	3.3	54.7
1.8288	26.53	537	8.6	8.35	0.9	4.8	55.8
2.7432	22.08	539	14.05	8.54	1.6	5	60.4
3.6576	15.82	535	20.72	8.69	5.7	4.9	58.8
4.572	10.94	523	26.92	8.89	10.5	13.8	64.4
4.93776	9.07	545	13.58	8.3	15.2	21.2	
5.12064	8.32	557	7.04	8.14	34.8	41.2	
5.27304	7.85	564	4.82	7.7	33.9	35.1	
5.42544	7.57	566	2.85	7.58	21.9	23.5	
5.4864	7.78	569	20.68	8.2	24.4	19.6	74.1
5.7912	6.54	572	0.62	7.44	10.9	13.3	
6.096	6.67	573	6.97	7.8	6.8	7	78.6
7.0104	6.18	577	5.87	7.64	5.6	9.1	-18.1
7.9248	5.79	550	3.08	7.57	3.5	6.8	-139.2
8.8392	5.58	583	1.86	7.52	3.6	6.3	-154.7
9.7536	5.49	590	1.3	7.47	6	6.6	-170.4
10.668	5.55	631	0.94	7.28	18.3	4.4	-200.9

July 22, 2013. 11:00 A.M.

Depth (m)	Temperature (°C)	DO (mg/l)	pH	Turbidity	Chlorophyll	Redox	Conductivity
0	28.61	7.17	8.07	0.3	3.1	34.7	531
0.9144	28.62	7.01	8.07	0.3	3.5	33.4	531
1.8288	28.54	6.92	8.03	0.4	3.7	32.7	532
2.7432	27.01	9.26	8.22	1	4.3	29.6	531
3.6576	20.36	17.73	8.41	1	3.9	29.2	541
4.572	14.58	22.99	8.52	2	7.5	31	531
5.4864	11.12	24.2	8.4	7.8	11.4	59.4	551
6.4008	7.6	5.41	7.55	18.3	18.8	-313.9	578
7.3152	6.36	1.14	7.29	4.4	8.1	-360	583
8.2296	5.94	0.96	7.25	3.9	6.7	-380.5	584
9.144	5.75	0.79	7.15	4.5	6.4	-373.5	589
10.0584	5.66	0.78	7.04	9.8	6.8	-372.6	613
5.9436	8.12	0.65	7.16	38.3	27.1		571
6.096	7.82	1.18	7.19	38.3	32.1		576
6.2484	7.49	0.7	7.17	17.8	17.9		574
5.7912	8.05	0.82	7.2	42.3	25		572

July 24, 2013. 10:00 A.M.

Depth (m)	Temperature (°C)	Conductivity	DO (mg/l)	pH	Turbidity	Chlorophyll	Redox
0	27.18	528	8.21	8.12	0.5	3.3	12.4
0.9144	27.18	527	8.07	8.12	0.5	3	14.8
1.8288	27.12	527	8.03	8.13	0.5	3.1	15.9
2.7432	25.41	530	12.84	8.36	1.4	4.5	17.2
3.6576	19.37	535	20.05	8.42	1.2	3.7	27.2
4.572	14.18	537	23.17	8.44	4.8	7.4	30.8
5.4864	10.38	560	19.51	8.21	20.5	15.6	43.6
5.7912	8.74	568	2.29	7.4	32.2	19.1	
5.9436	8.41	568	2.14	7.33	38.3	35	
6.096	7.78	571	1.4	7.3	23.2	20.4	-150.5
7.0104	6.49	578	1.05	7.28	5.8	9.3	-228.8
7.9248	5.97	581	0.95	7.26	3.9	6.6	-238.4
8.8392	5.71	586	0.85	7.11	4.6	7.1	-251
9.7536	5.69	605	0.83	7.06	7	6.6	-260.3
10.668	5.73	633	0.83	6.85	21.3	9.4	-265.6

August 7, 2013. 11:00 A.M.

Depth (m)	Temperature (°C)	Conductivity	DO (mg/l)	pH	Turbidity	Chlorophyll	Redox	Eh
0	26.03	519	9.11	8.27	0.5	3.4	72.8	272.8
0.9144	25.72	519	9.28	8.19	0.5	2.9	75.1	275.1
1.8288	25.5	518	9.16	8.18	0.6	2.6	102.9	302.9
2.7432	24.87	520	9.24	8.15	0.7	3.1	43.3	243.3
3.6576	21.64	529	14.76	8.28	0.9	3.4	42.4	242.4
4.572	15.64	530	21.95	8.43	1.1	3.4	41.1	241.1
5.4864	10.59	553	22.69	8.42	8	9.3	-65	135
5.7912	9.63	563	17.6	8.13	22.9	15.2	-52.8	147.2
6.096	9.02	569	14.95	7.93	47.4	27.2	-58.4	141.6
6.15696	8.3	567	5.65	7.56	47.8	36		200
6.4008	7.64	572	1.31	7.31	20.8	24.6	-119.9	80.1
7.3152	6.42	579	0.72	7.28	4.7	9.7	-168.5	31.5
8.2296	6.1	580	0.64	7.27	3.9	7	-216.4	-16.4
9.144	5.81	590	0.59	7.2	5.3	7	-234.3	-34.3
10.0584	5.76	617	0.6	7.08	8.8	7.5	-247.5	-47.5
10.9728	5.82	688	0.6	6.9	24.9	10.3	-257.5	-57.5

August 13, 2013. 2:00 P.M.

Depth (m)	Temperature (°C)	Conductivity	DO (mg/l)	pH	Turbidity	Chlorophyll	Redox
0	27.76	528	9.66	8.17	0.6	2.7	72.2
0.9144	27.69	528	9.51	8.2	0.5	2.6	73.7
1.8288	26.91	529	9.53	8.19	0.6	3	76.7
2.7432	24.83	534	11.2	8.26	0.7	2.8	82.1
3.6576	21.24	541	18.11	8.33	1.2	4.2	90.8
4.572	15.51	545	23.9	8.51	1.1	3.5	112.8
5.4864	11.45	557	24.33	8.58	4.8	7.1	111.8
5.7912	10.16	571	21.64	8.36	14.1	10.5	89.4
6.096	9.18	581	16.39	7.99	47.8	25.9	-12.1
6.2484	8.82	582	3.68	7.56	54.9	40	
6.4008	7.83	585	0.73	7.34	46.1	42.6	-191.4
6.5532	7.64	586	0.78	7.34	11.9	26.7	
7.3152	6.83	592	0.85	7.31	6	14.5	-210.6
8.2296	6.12	597	0.75	7.3	4.2	8.3	-221.3
9.144	5.82	604	0.69	7.26	5.2	6.8	-233.6
10.0584	5.82	642	0.69	7.1	10.7	7.9	-250.6
10.9728	5.87	696	0.69	6.93	19.2	10	-264.7

October 2, 2013. 1:00 P.M.

Depth (m)	Temperature (°C)	Conductivity	DO (mg/l)	pH	Turbidity	Chlorophyll	Redox
0	20.66	521	8.92	8.16	-0.4	2.7	81.3
0.9144	20.13	520	8.94	8.27	-0.3	2.7	80.9
1.8288	20.02	520	8.82	8.3	-0.3	2.7	83
2.7432	19.92	520	8.74	8.32	-0.2	3	83.6
3.6576	19.7	521	8.71	8.33	-0.2	2.5	83.4
4.572	18.11	540	10.04	8.29	0	3.2	84.72
5.4864	14.32	567	11.02	8.24	1.8	4.5	85.3
6.4008	10.25	576	2.02	7.81	12.9	11.8	88
6.7056			0.44				66.3
6.97992	8.77	583	0.3	7.61	22.8	107	-141.3
7.28472	8.09	585	0.21	7.5	31.7	219	-162.6
8.2296	6.82	595	0.15	7.45	7.7	21.8	-183.1
9.144	6.31	613	0.17	7.38	5.8	13.3	-185.9
10.0584	6.14	659	0.14	7.24	8.2	11.9	-189.1

CRYSTAL LAKE ANALYTICAL DATA

PHOSPHORUS

May 24, 2013.

Depth (m)	absorbance	concentration (mg/L PO_4^{3-})
0	0.05	0.053335
0.9144	0.24	0.241948
1.8288	0.34	0.341218
2.7432	0.25	0.251875
3.6576	0.26	0.261802
4.572	0.48	0.480196
4.8768	0.02	0.023554
5.1816	0.03	0.033481
5.4864	0.03	0.033481
5.7912	0.03	0.033481
6.7056	0.06	0.063262
7.62	0.53	0.529831
8.5344	1.24	1.234648
9.4488	0.25	0.251875
10.3632	0.31	0.311437

August 7, 2013.

Depth (m)	absorbance	concentration (mg/L PO_4^{3-})
0	0.28	0.281656
1.8288	0.21	0.212167
3.6576	0.11	0.112897
5.4864	0.25	0.251875
5.7912	0.16	0.162532
6.096	0.02	0.023554
6.4008	0	0.0037
8.2296	0.14	0.142678
10.0584	1.22	1.214794

October 2, 2013.

Depth (m)	absorbance	concentration (mg/L PO_4^{3-})
0	1.18	1.175086
1.8288	0.57	0.569539
3.6576	0.47	0.470269
5.4864	0.72	0.718444
6.7056	0.74	0.738298
7.0104	0.89	0.887203
7.3152	0.76	0.758152
8.2296	1.07	1.065889
10.0584	1.43	1.423261

SILICA

May 24, 2013.

Depth (m)	concentration (mg/L)
0	0.174
0.9144	0.195
1.8288	0.185
2.7432	0.166
3.6576	0.083
4.572	0.082
4.8768	0.077
5.1816	0.09
5.4864	0.11
5.7912	0.128
6.7056	0.196
7.62	0.322
8.5344	0.298
9.4488	0.4
10.3632	0.548

August 7, 2013.

Depth (m)	concentration (mg/L)
0	0.4
1.8288	1.8
3.6576	1.9
5.4864	1.2
5.7912	0.7
6.096	0.8
6.4008	0.7
8.2296	1.9
10.0584	3

October 2, 2013.

Depth (m)	concentration (mg/L)
0	2.2
1.8288	1.1
3.6576	1.5
5.4864	1.8
6.7056	1.4
7.0104	2.7
7.3152	2.2
8.2296	2.7
10.0584	5.3

SULFATE

May 24, 2013.

Depth (m)	Concentration (mg/L)
0	7.2344374
0.9144	7.3080808
1.8288	7.1400112
2.7432	7.0053748
3.6576	7.6315696
4.572	7.6830748
5.4864	7.4418136
6.096	7.6365394
6.4008	7.6234372
6.7056	7.5308182
7.0104	7.477054
7.62	7.3094362
8.5344	7.4991922
9.4488	7.635184
10.3632	6.8178778
11.2776	7.2909124

August 7, 2013.

Depth (m)	Concentration (mg/L)
0	5.708257
1.8288	6.069697
3.6576	6.187165
5.4864	6.1749664
5.7912	6.5630626
5.9436	6.4776724
6.4008	6.2901754
7.3152	5.7819004
8.2296	5.5745242
9.144	3.6308806
10.0584	1.1062222

October 2, 2013.

Depth (m)	Concentration (mg/L)
0	5.3499796
1.8288	5.3075104
3.6576	5.3233234
5.4864	5.218054
6.7056	5.6490712
7.0104	5.3179018
7.3152	4.906312
8.2296	4.8877882
10.0584	0.006541

SULFIDE

May 24, 2013.

Depth (m)	Concentration (mg/L)
0	0
0.9144	0
1.8288	0
2.7432	0
3.6576	0
4.572	0
5.4864	0
6.096	0
6.4008	0
6.7056	0
7.0104	0
7.62	0
8.5344	0.02
9.4488	0.03
10.3632	0.04
11.2776	0.06

August 7, 2013.

Depth (m)	Concentration (mg/L)
0	0
1.8288	0
3.6576	0
5.4864	0
5.7912	0
5.9436	0
6.4008	0.25
7.3152	1.375
8.2296	2.5
9.144	5.875
10.0584	9.25

October 2, 2013.

Depth (m)	Concentration (mg/L)
0	0
1.8288	0
3.6576	0
5.4864	0
6.7056	0
7.0104	0.5
7.3152	1.875
8.2296	8.125
10.0584	13

SULFATE ISOTOPIC ANALYSIS

May 24, 2013.

Depth (m)	Composition (‰)
0	1.8
0.9144	1.6
1.8288	1.9
2.7432	1.8
3.6576	1.7
4.572	1.7
5.4864	1.4
6.096	1.6
6.4008	1.5
6.7056	1.6
7.0104	1.6
7.62	1.7
8.5344	1.5
9.4488	2.0
10.3632	3.4
11.2776	5.6

August 7, 2013.

Depth (m)	Composition (‰)
0	2.1
1.8288	2.1
3.6576	2.0
5.4864	1.9
5.7912	1.8
5.9436	1.6
6.4008	2.8
7.32	5.344855967
8.23	7.841426612
9.14	10.33799726
10.06	12.86200274

October 2, 2013.

Depth (m)	Composition (‰)
0	2.0
1.8288	2.2
3.6576	2.1
5.4864	2.2
6.7056	2.3
7.0104	2.6
7.3152	3.7
8.23	7.001082642
10.06	13.60519668

SULFIDE ISOTOPIC ANALYSIS

May 24, 2013.

Depth (m)	Composition (‰)
9.4488	-14.7
10.3632	-13.6

August 7, 2013.

Depth (m)	Composition (‰)
8.2296	-17.4
10.0584	-1.7

October 2, 2013.

Depth (m)	Composition (‰)
7.3152	-20.9
8.2296	-17.7
10.0584	0.3

***PLANKTOTHRIX RUBESCENS* ISOTOPIC ANALYSIS**

Sample Date	Depth (m)	$d^{34}S$ (‰)
8/7/2013	6.1	-0.15
10/2/2013	7.2	0.48

VI. REFERENCES

1. "2009 Environmental Results." United States Environmental Protections Agency. 2009. Web. 19, Nov. 2014. <http://www.epa.gov/airmarkets/progress/ARP09_3.html>

2. Arenschield, Laura. "Buckeye Lake algae cause for worry." Dayton Daily News, 2014.

3. Brown, T.; Simpson, J.. "Managing Phosphorus Inputs Into Lakes I: Determining the Trophic State of Your Lake." Watershed Protection Techniques. Center for Watershed Protection, Ellicott City, MD, 2001; 3 (4): 771-781

4. Carmody, Rebecca W.; Plummer, L. Niel; Busenberg, Eurybiades; Coplen, Tyler B. "Methods for collection of dissolved sulfate and sulfide and analysis of their isotopic composition." U.S. Geological Survey, Reston, Virginia, 1998.

5. Chaudhary, Anita; Haack, Sheridan Kidd; Duris, Joseph W.; Marsh, Terrence L. "Bacterial and Archaeal Phylogenetic Diversity of a Cold Sulfur-Rich Spring on the Shoreline of Lake Erie, Michigan." Applied and Environmental Microbiology, 2009.

6. Cheng, Songlin. Personal communication, 2014.

7. Christiansen, Guntram; Kurmayer, Rainer; Liu, Qian; Borner, Thomas. "Transposons Inactivate Biosynthesis of the Nonribosomal Peptide Microcystin in Naturally Occurring *Planktothrix* spp." Applied and Environmental Microbiology, 2006.

8. Collins, Molly. "Hydrogeochemistry and hydrogeology near Crystal Lakes, Clark County, Ohio." Masters Thesis, Wright State University, Dayton, Ohio, 1999; p 90.

9. Dahl, Christiane; Hell, Rudiger; Leustek, Thomas; Knaff, David. "Introduction to Sulfur Metabolisms in Phototrophic Organisms." Sulfur Metabolism in Phototrophic Organisms, 2008; 1-14.

10. Dunnette, David A.; Chynoweth, David P.; Mancy, Khalil H. "The Course of Hydrogen Sulfide in Anoxic Sediment." Pergamon Press Ltd, Water Res., 1985; 19,7,875-884.

11. Figueiredo, Daniela R.; Azeiteiro, Ulisses M.; Esteves, Sonia M.; Goncalves, Fernando J.M.; Pereira, Mario J. "Microcystin-producing blooms- a serious global public health issue." Elsevier, Ecotoxicology and Environmental Safety, 2004; 59, 151-163.

12. Fry, B.; Silva, S.R.; Kendall, C.; Anderson, R.K. Oxygen isotope corrections for online $d^{34}S$ analysis. Rapid Communications in Mass Spectrometry, 2002; 16, 854-858.

13. Garlick, S.; Oren, A.; Padan, E. "Occurrence of Facultative Anoxygenic Photosynthesis Among Filamentous and Unicellular Cyanobacter." Journal of Bacteriology, 1977.

14. Gemerden, Hans Van; Mas, Jordi. "Ecology of Phototrophic Sulfur Bacteria." Anoxygenic Photosynthetic Bacteria, 1995; 49-85.

15. Giordano, Mario; Norici, Alessandra; Ratti, Simona; Raven, John A. "Role of Sulfur for Algae: Acquisition, Metabolism, Ecology and Evolution." Sulfur Metabolism in Phototrophic Organisms, 397-415, 2008.Goldthwait, R. "The Water Resources of Clark County, Ohio, State of Ohio, Department of natural Resources, Division of Water, Bulletin 22, Columbus, Ohio, 1952; pp. 46, 56.

16. Groot, P. de. "Handbook of Stable Isotope Analytical Techniques." Elsevier, Amsterdam ; London, 2004.

17. Halstvedt, Camilla Blikstad; Rohrlack, Thomas; Andersen, Tom; Skulberg, Olav; Edvardsen, Bente. "Seasonal dynamics and depth distribution of *Planktothrix* spp. In Lake Steinsfjorden (Norway) related to environmental factors." Journal of Plankton Research, 2007; 29(5), 471-482.

18. Hammerschmidt, Chad. Personal communication, 2014.

19. Hell, Rudiger. *Sulfur Metabolism in Phototrophic Organisms.* Advances in Photosynthesis and Respiration, 2008; p 27.

20. Hicks, B. B. "On the assessment of atmospheric deposition of sulfur and nitrogen species to the surface of large inland lakes - Lake Champlain." Res. J. Great Lakes, 2007; **33,** 114-121.

21. Hoefs, Jochen. "Stable Isotope Geochemistry." Minerals in Rocks, Springer-Verlag, 1987.

22. Jedrysek, Mariusz O. "Sulphate reduction – methane oxidation: A potential role of this process in the origin of C isotope environmental record in freshwater carbonates." Polish Geological Institute Special Papers, 2005; 16, 18-34.

23. Komárek, Jiří; Komárková, Jaroslava. "Taxonomic review of the cyanoprokaryotic genera *Planktothrix* and *Plaktothricoides*." Czech Phycology, Olomouc, 2004.

24. Konopka, A; Klemer, A. R.; Walsby, A. E.; Ibelings, B. W. "Effects of macronutrients upon buoyancy regulation by metalimnetic *Oscillatoria agardhii* in Deming Lake, Minnesota." Journal of Plankton Research, Bol. 1993; 15(9), 1019-1034.

25. Lampert, W.; Sommer, U. "Limnoecology: the ecology of lakes and streams." Oxford University Press, New York, 1997.

26. Legnani, Elena; Copetti, Diego; Oggioni, Alessandro; Tartari, Gianni; Palumbo, Maria Teresa; Morabito, Giuseppe. "*Plaktothrix rubescens'* seasonal dynamics and vertical distribution in Lake Pusiano (North Italy)." Journal of Limnology, 2005; 64(1), 61-73.

27. Miklasz, Kevin A.; Denny, Mark W. "Diatom sinking speeds: Improved predictions and insight from a modified Stokes' law." Limnol. Oceanogr., 2010; 55(6), 2512-2525.

28. Norris, S.; Goldthwait, R.; Cross, W.; Sanderson, E. "The Water Resources of Clark County, Ohio. State of Ohio, Department of Natural Resources, Division of Water, Bulletin 22. Columbus, Ohio, 1952; 82 p.

29. Obrien, D.; Birkner, F. Kinetics of Oxygenation of Reduced Sulfur Species in Aqueous-Solution. Environ. Sci. Technol, 1977; **11,** 1114-1120.

30. Pai, S.; Yamg, C.; Riley, J. Effects of acidity and molybdate concentration on the kinetics of the formation of the phosphoantimonylmolybdenum blue complex. Analytica Chimica Acta, 229 (1990): 1990; 15-120.

31. Wigley, T.M.L.; Plummer, L.N.; Pearson, F.J. "Mass transfer and carbon isotope evolution in natural water systems." Geochimica et Cosmochimica Acta 42, 1978; 1117-1139.

32. Rabalais, Nancy N.; Turner, R. Eugene; Wiseman, William J. Jr. “Gulf of Mexico Hypoxia, A.K.A. ‘The Dead Zone’.” Annu. Rev. Ecol. Syst., 2002; 33, 235-263.

33. Rudnicki, Mark D.; Elderfield, Henry; Spiro, Baruch. "Fractionation of sulfur isotopes during bacterial sulfate reduction in deep ocean sediments at elevated temperatures." Geochimica et Cosmochimica Acta, 2001; 65, 5, 777-789.

34. Sadurski, Stephen. “The Biogeochemistry of Carbon Isotopes in Local Lakes.” Master’s Thesis, Wright State University, Dayton, Ohio, 2012.

35. Sarazin, Gerard; Michard, Gil; Prevont, Francois. “A rapid and accurate spectroscopic method for alkalinity measurements in sea water samples.” Water Research, 1999; 33:290-294.

36. Scavia, Donald; Allan, J. Davis; Arend, Kristin K.; Bartell, Steven; Beletsky, Dmitry; Bosch, Nate S.; Brandt, Stephen B.; Briland, Ruth D.; Daloglu, Irem; DePinto, Joseph V.; Dolan, David M.; Evans, Mary Anne; Farmer, Troy M.; Goto, Daisuke; Han, Haejin; Hook, Tomas O.; Knight, Roger; Ludsin, Stuart A.; Mason, Doran; Michalak, Anna M.; Richards, R. Peter; Roberts, James J.; Rucinski, Daniel K.; Rutherford, Edward; Schwab, David J.; Sesterhenn, Timothy M.; Zhand, Hongyan; Zhou, Yuntao. “Assessing and addressing the re-eutrophication of Lake Erie: Central basin hypoxia.” Journal of Great Lakes Research, Elsevier. 2014; 40, 226-246.

37. Senese, Fred. “How can I predict oxygen solubility in water?” General Chemistry Online, Frostburg State University, Maryland, 1997.

38. Shaw, Byron; Mechenich, Christine; Klessig, Lowell. “Understanding Lake Data.” Board of Regents of the University of Wisconsin System, 2004.

39. Smith, V., G. Tilman and J. Nekola. Eutrophication: impacts of excess nutrient inputs on freshwater, marine, and terrestrial ecosystems. Environ. Pollut., 1999; **100,** 179-196.

40. Sorvari, Sanna. “Climate Impacts on Remote Subarctic Lakes in Finnish Lapland: Limnological and Paleolimnological Assessment with a Particular Focus on Diatoms and Lake Saanajarvi.” Thesis, University of Helsinki, 2001.

41. “Sources and Solutions.” United States Environmental Protection Agency. N.p., 16 Mar. 2014. Web. 27 Aug. 2014. <http://www2.epa.gov/nutrientpollution/sources-and-solusions>

42. Stewart, R. Acid Rain and Acid Deposition. Environmental Science in the 21st Century- an Online Textbook. 2012.

43. Talsna, A.; J. Lazorchak. Water quality investigations on Crystal Lakes (Near Medway, Ohio, Clark County), 1975.

44. Thode, H. G. "Sulphur Isotopes in Nature and the Environment: An Overview." Stable Isotopes in the Assessment of natural and Anthropogenic Sulphur in the Environment, SCOPE, 1991.

45. Vaccari, D. Standard methods for the examination of water and wastewater. *CHOICE*: Current Reviews for Academic Libraries, 2012; 12, 2316.

46. Van den Wyngaert, Silke; Salcher, Michaela M.; Pernthaler, Jakob; Zeder, Michael; Posch, Thomas. "Quantitative dominance of seasonally persistent filamentous cyanobacteria (*Planktothrix rubescens*) in the microbial assemblages of a temperate lake." American Society of Limnology and Oceanography, Inc., 2011.

47. Wetzel, Robert G. "Limnology: Lake and river ecosystems" San Diego: Academic Press., 2001; p. 1006.

48. Wisebaker, April. "The impact of nutrient availability and algal community on carbon isotope fractionation in Crystal lake, Clark County, Ohio." Masters Thesis, Wright State University, Dayton, Ohio. 2008.

49. Woodruff, M. "Isotope geochemistry of oxygen, hydrogen and carbon in Crystal Lakes, Medway, Clark County, Ohio." Thesis, Wright State University, 1999.

50. Yang, X. E.; X. Wu; H. L. Hao; Z. L. He. Mechanisms and assessment of water eutrophication. J. Zhejiang University, 2008; **9,** 197-209.